CERN LIBRARIES, GENEVA

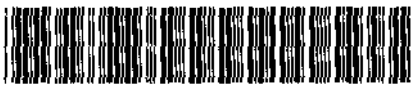

CM-P00046548

CERN/SPSC/80-96
SPSC/M 255
Date: September 1st 1980

Ref.:

M E M O R A N D U M

Copy to/Copie à:

To/A : Members of the SPS Committee

From/De : UA2 Collaboration

Subject/: Objet : Cogne meeting of the SPSC

The enclosed set of documents aims at answering your request for information concerning UA2. It includes :

i) a copy of a note prepared for the recent Uppsala Conference and describing briefly the main features of the detector,

ii) a short time table of the detector construction and installation in LSS4,

iii) a brief summary of the capability of the experiment to tackle various physics questions.

Information contained in documents CERN/SPSC/78-8 P93, 78-54/P93/Add.1, 78-126/M139 and 78-133/M141 is still valid and can be used as a basis to assess the merits of our proposed experiment.

Jean Marc Gaillard will take part in the Cogne meeting as a member of the SPS Committee. He has been given authority to speak in the name of the Collaboration in case you would need any further information.

A DETECTOR TO STUDY $p\bar{p}$ INTERACTIONS AT THE SPS-COLLIDER

The UA2 Collaboration

University of Bern
K. Borer
B. Hahn
H. Hänni
J. Schacher
W. Zeller

CERN
F. Bonaudi
M. Borghini
A. Clark
P. Darriulat
L. DiLella
O. Gildemeister
T. Himel
V. Hungerbühler
P. Jenni
G. Parrour
J. Ringel
A. Rothenberg

Niels Bohr Institute Copenhagen
B. Madsen
R. Møllerud
J. Dines Hansen
P. Hansen
O. Kofoed Hansen

LAL, Orsay
J.C. Chollet
L. Fayard
D. Froidevaux
J-M. Gaillard
B. Merkel
H. Plothow
J-P. Repellin
G. Sauvage

Istituto di Fisica Nucleare, Pavia
C. Conta
M. Fraternali
G. Goggi
F. Impellizzeri
M. Livan
G.C. Mantovani
F. Pastore

DPHPE, CEN Saclay
M. Banner
C. Bruneton
S. Loucatos
B. Mansoulié
P. Perez
J. Teiger
H. Zaccone
A. Zylberstejn

Abstract :

A detector is being constructed to study $p\bar{p}$ interactions at the SPS-collider. Its principal aim is to detect the production and decay of $W^{\pm}$ and Z^{o} bosons. The design combines large solid angle coverage with compactness and simplicity of operation. It includes electromagnetic and hadronic calorimetry in the central region and magnetic spectrometers in the forward and backward cones equipped for electron detection. A high resolution vertex detector provides an accurate measurement of the event topology. In addition a small azimuthal wedge in the central region is instrumented to explore new aspects of $p\bar{p}$ interactions at very high energies.

1 - GENERAL OVERVIEW

Physics interest. The injection of cooled antiprotons into the SPS and their acceleration to 300 GeV opens up the possibility of studying $p\bar{p}$ collisions at a centre-of-mass energy $\sqrt{s}$ = 600 GeV where many new phenomena are expected to occur.

In particular with a luminosity $L \cong 10^{30}$ cm^{-2} s^{-1} it becomes possible to produce a significant number of $W^{\pm}$ and Z^{o}, the weak intermediate bosons of unified gauge theories, if their production cross section is of the order of a few 10^{-33} cm^2 as predicted by current QCD calculations.

In the Weinberg Salam model, with $\sin^2 \Theta_w = .23$ the masses of the gauge bosons are $m_{Zo} = 89$ GeV/c^2 and $m_W = 78$ GeV/c^2 and their branching fractions into the electron channels $Z^o \to e^+e^-$ and $W^{\pm} \to e^{\pm}\upsilon$ are 3% and 8% respectively.

The V-A coupling of the W's to quark and lepton doublets is expected to result in a strong forward-backward decay asymmetry.

The experimental apparatus. The detector is largely dedicated to the observation of the hadronic and leptonic decay modes of the weak vector bosons ($W^{\pm}$, Z^o). Nevertheless, the resulting apparatus is very suitable for the detection of other expected -or unexpected- phenomena.

A constant and major concern has been to maintain simplicity and compactness in the design, as imposed by the constraint of operating the detector in the difficult environment of the SPS tunnel.

For this reason, and because of the good energy resolution obtainable in lead-scintillator sandwich counters, we have concentrated on the electron rather than the muon decay modes of the $W^{\pm}$ and Z^o. Electron identification is therefore instrumented over nearly 4π sr by lead-scintillator sandwich counters.

A drawing of the entire detector is presented in Fig. 1.1. The photographs of a 1 : 10 scale model (Fig. 1.2 ; only one of the forward detectors is shown) give a perspective view of the detector in its symmetric configuration (above, with forward detector recessed) and in the "wedge"

configuration (below). At the centre of the apparatus is the vertex detector, a system of cylindrical proportional and drift chambers, that will measure particle trajectories in a region free of magnetic fields. This detector is under construction at LAL, Orsay. In the central region, covering ±1 rapidity unit about 0, the vertex detector is surrounded by lead-scintillator sandwich counters followed by hadron calorimeters. The extension of hadron identification to forward angles was not considered, because it would need the addition of very voluminous and expensive calorimeter elements.

As noted above, an electron-positron asymmetry in the W-decay is expected in some models, with a significant signal between 20° and 30°. Our apparatus measures this asymmetry. The angular range to cover, and the angular dependence of the electron energy (harder electrons at smaller angles) indicate a toroidal field as a suitable configuration to perform the charge measurement. The polar angular regions of 20° to 37.5° and 142.5° to 160° are each instrumented with a toroidal magnet consisting of 12 coils. The average field integral along particle trajectories is .38 Tm. Each region between two adjacent toroid coils is followed by a set of 9 drift chamber planes with an average lever arm of 80 cm. Together with the vertex detector, these forward/backward (F/B) chambers allow reliable charge measurements on electrons up to 60 GeV/c transverse momentum. The F/B drift chambers are being built at NBI, Copenhagen, and at the Istituto di Fisica Nucleare in Pavia. Each drift chamber set is followed by a converter of 6mm Pb and proportional tubes for an accurate measurement of the position of electromagnetic showers. This allows an improved rejection of the overlap background (a low momentum hadron track near a π^0, simulating an electron in the calorimeter that follows) and a better hadron rejection. The tubes are constructed at the University of Bern. The proportional tubes are followed by the F/B calorimeters, consisting of lead scintillator sandwiches and covering the same solid angle as the toroid magnets. The F/B calorimeters are built by CEN, Saclay.

The detector is blind below 20° causing the loss of some $W^{\pm}$ and Z^{o} decays. However the identification of electrons in this region would in any case have been made more difficult by higher particle densities,

higher average particle energies, and beam-halo background.

The momentum measurement of charged secondaries in the central region would permit the measurement of charged particle inclusive production, and greatly benefit the study of jet structure at large transverse momentum, free quark production, etc... To this end a 30° azimuthal window will be opened in the calorimeter in the first phase of operation of the detector and equipped as a magnetic spectrometer. The use of the calorimeter iron as the return yoke of the magnetic spectrometer allows a very compact geometry. Electron identification remains possible in this azimuthal wedge because of the presence of a large lead-glass wall behind the magnetic spectrometer. The field integral is of the order of 1 Tm and charged particle trajectories are measured in a set of 12 large drift chamber planes. This "wedge detector" is composed of elements left over from a previous CERN-Saclay experiment at the ISR.

In the symmetric configuration the total acceptance is ≅ 63% for $Z^o \to e^+e^-$ and ≅ 75% for $W^\pm \to e^\pm \nu$; it is independent of the p_T-distribution of the produced boson, up to at least $\langle p_T \rangle$ = 10 GeV/c. Thus, with a Z^o production cross section of 2 x 10^{-33} cm^2 and the leptonic branching ratio mentioned above, .14 detected $Z^o \to e^+e^-$ per operating hour are expected. The mass resolution at the Z^o peak is expected to be ≅ 1.5%.

Trigger and data acquisition. To trigger on the electronic decays of the intermediate vector bosons, only the electromagnetic calorimeters are used. The pulse-heights of 4 adjacent calorimeter elements are linearly added and integrated. The trigger then consists of requiring two such energy clusters above some minimum p_T-threshold or one above a higher threshold. The background comes mainly from the neutral component of jets, whose p_T spectrum drops sharply. Thus, we expect to be able to keep the trigger rate near 1/sec without any significant loss of W or Z events by setting the thresholds in the 10 GeV/c p_T-range. Other triggers are being designed, such as very large amounts of electromagnetic or hadronic energy deposited in the entire calorimeter, large particle multiplicity etc...

The data acquisition will be done through a VAX 11/780 computer. Four other minicomputers will be available for parallel detector testing before runs and for in-depth monitoring during data-taking.

2 - THE CENTRAL CALORIMETER

Structure. The central calorimeter consists of electromagnetic (EM) and hadronic calorimeters which cover polar angles from 40° to 140° and the full azimuthal range. In a first phase a 60° azimuthal wedge is replaced by a magnetic spectrometer for exploratory studies. The calorimeter assembly consists of 240 independent cells, each cell covering 15° in azimuthal and 10° in polar angle. This is a compromise between minimizing dead space and providing sufficient space resolution. The details of an individual cell are shown in Fig. 2.1. The EM compartment contains a stack of 26 lead plates (3.5 mm thick) and 27 NE104 scintillator plates (4 mm thick). The hadronic calorimeter is divided into 2 compartments. Hadron 1 and Hadron 2 contain respectively 18 and 22 pairs of iron plates (15 mm thick) and scintillator plates (5 mm thick PMMA based scintillator with 10% naphtalene, 1% PBD, and 0.01% POPOP). To minimize dead space, light is collected with BBQ wavelength shifting light guides ; they are doped with 80 mg of BBQ per liter. Each compartment is viewed with 2 light guides and 2 photomultipliers to provide information on the position of the shower so that light collection efficiency corrections can be made. In addition the last 3 scintillator plates are viewed with a 2 cm diameter BBQ rod placed in a hole in the center of the cell. This "backtag" readout is intended to tag energy escaping out the back of the cell. Philips XP 2008 phototubes are used for all compartments but the EM which uses XP2012's.

Mechanically the whole calorimeter is built up of 24 modules (orange slices) each of which covers 15° of azimuth. The iron plates of 10 hadron calorimeter cells are screwed between 2 support sheets of 5 mm thickness to form an orange slice. Ten independent self supporting EM calorimeter cells are mounted to each orange slice. There is less than 2 mm dead space between EM cells.

Calibration. At the $p\bar{p}$ collider we expect to have no source of particles of known momentum which could be used to calibrate the calorimeter cells. Thus each cell must be calibrated (obtain number of picocoulombs per GeV) in a test beam and there must be a system to monitor changes of gain (of photomultipliers and ADC's). A system of xenon flashers and vacuum tube photodiodes is used for this purpose. Each calorimeter slice is equipped with two xenon flash lamps and three photodiodes. Light from one flasher is sent via Fort SP01 plastic optical fibres to small pieces of BBQ attached to each light guide. In this way light with the same spectrum as that from the calorimeter is delivered to the photomultipliers. Light from the other flasher goes via optical fibers through scintillators of the EM compartments to the BBQ light guides and the photomultipliers. This second system is sensitive to attenuation changes of the scintillator. Light from both flashers is sent to three EMI-PD1900 vacuum tube photodiodes which monitor the intensity of the flashes. These photodiodes are expected to have a gain constant to better than a percent over a period of years. Three diodes are used so the malfunctioning of one can be detected and corrected. With this system an amount of light whose time variations are measured by the photodiodes, can be delivered to all photomultipliers allowing their gains to be monitored.

The pulse heights of minimum ionizing particles coming from the $p\bar{p}$ collider will be used as another monitor of gain drifts.

Prototype test results. Measurements have been made with a prototype module in a test beam to determine the properties of the calorimeter cells. The data presented here are only preliminary.

The energy resolution as a function of energy for electrons and hadrons normally incident on the center of a cell is shown in Fig. 2.2. For the electron data, $\sigma/\sqrt{E}$ is nearly constant at 0.155. For the hadron data it increases with energy. This is caused primarily by particles escaping out the back of the calorimeter which is only 4.5 absorbtion lengths thick. The relative amounts of energy deposited in the Hadron 1, Hadron 2, and the backtag compartments can be used to eliminate events

with a lot of energy escaping. This improves $\sigma/\sqrt{E}$ to 0.54 at 10 GeV when 16% of the events are cut out and to 0.60 at 40 GeV when 40% of the events are cut out. At the $p\bar{p}$ collider single hadrons with energies over 40 GeV are expected to be very rare so this energy escape is not a large problem.

The response to 40 GeV electrons for the third largest cell as a function of distance from the BBQ light guide is shown in Fig. 2.3. The curves for the two BBQ's are different because one is on the large side and one is on the small side of the trapezoidal cell. We expect to be able to correct for this variation in light collection efficiency (caused by the cell geometry and absorption in the scintillator) to better than 1%. The sharp drop off near the BBQ is due to energy escaping into the adjacent cell.

Electronics. All photomultiplier signals go through 85 m long 96 CEI-50Ω coax cables to a unity gain buffer and are digitized with a Lecroy 2280 ADC system. Phototube high voltages are set so that a p_T of 80 GeV/c corresponds to ADC channel 4000. The EM signals are, in addition to the unity gain signal, also amplified by a factor of 12 and recorded in separate ADC channels so that the minimum ionizing peak can be seen, in about channel 100. These buffers and amplifiers also make signals available to the trigger logic for use in generating the electron pair mass and high p_T trigger.

3 - WEDGE SPECTROMETER

The role of this spectrometer is to measure charged particle and π^o momenta over a limited solid angle. A 60° azimuthal opening in the central calorimeter is obtained by removing 4 calorimeter slices (Fig. 3.1). Two magnet coils, closely fitting the iron cross-section of the calorimeter (used for the field return), produce an average field integral of 1 Tm.

The spectrometer is equipped with 12 drift chamber planes, 2 scintillator hodoscopes and a leadglass calorimeter. Each drift chamber of 3.2 m × 1 m dimension is equipped with 128 sense wires, grouped in pairs

to resolve the left-right ambiguity. The spatial resolution of these chambers is about 150 μm ; together with the vertex detector and the magnetic field, this is expected to result in a momentum resolution of about $\Delta p/p = 2 \times 10^{-2} p$. The first hodoscope consists of 28 scintillators, each equipped with 2 photomultipliers ; it will measure time-of-flight together with the hodoscope of the vertex detector. The second hodoscope which is separated from the first by a 2 cm thick iron plate, consists again of 28 scintillators, each with one phototube ; it is used as a shower counter. The hodoscopes are followed by a leadglass wall, 28 blocks wide by 10 blocks high. Each block is 15 cm wide by 15 cm high and 35 cm (14 radiation lengths) deep.

At the nominal distance of 3 m from the interaction region, the wedge detector subtends ±35 degrees about 90° in Θ, and ±14 degrees about the horizontal in $\emptyset$. It can be recessed to a distance of 5 m, so that the 2 gammas from neutral pions of up to 2.4 GeV/c can be resolved.

4 - THE VERTEX DETECTOR

The vertex detector is built at the Laboratoire de l'Accélérateur Linéaire (L.A.L.) in ORSAY. Its aim is to determine with a high precision the coordinates of the interaction vertex and to measure the directions of all charged particles. It consists of 4 multiwire proportional cylindrical chambers (MWPC - C1 to C4) with cathode strip readout, 2 Jade type drift chambers (JC1, JC2) with charge division and multihit readout, a scintillator hodoscope (VH) and a 5th MWPC (C5) with 1.5 radiation lengths of Tungsten (W) in front (see fig.4.1 for the vertical cut along the beam and fig.4.2 for the transverse cut normal to the beam). The smallest chamber C1 has a diameter of 20 cm and a length of 112 cm. The maximum diameter is 71 cm for chamber C5. The longest chamber is C4, it's length is 188 cm. The vertex detector covers 2 π in ϕ and 20° to 160° in θ . A combination of the two types of chambers has been chosen, because one can achieve a good measurement of a track along the beam (σ = 200 μ) by determining the centroid of the charge distribution on the cathode strips, whereas the orthogonal ϕ coordinate is measured with a good accuracy by the jet chambers (σ = 200μ). The expected resolution for the vertex determination is therefore 200 μ in all 3 projections.

4.1.1 - Mechanics of the strip chambers C1 - C5

Each MWPC consists of an internal and an external self supporting cathode strip cylinder and proportional wires parallel to the cylinder axis in between. Each cathode strip cylinder is made of 25 μ (+ 300 Å Al) aluminized Kapton, 1 mm Rohacell (C1 and C2 0.5 mm), 25 μ Kapton, 1 mm Rohacell (C1 and C2 0.5 mm) and 50 μ Kapton with 10 μ silver coating for the strips (see graph below).

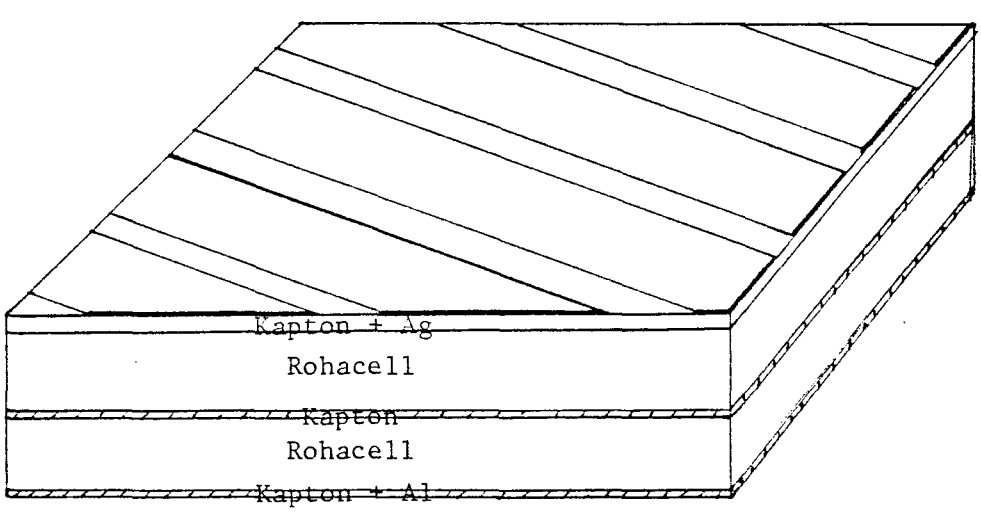

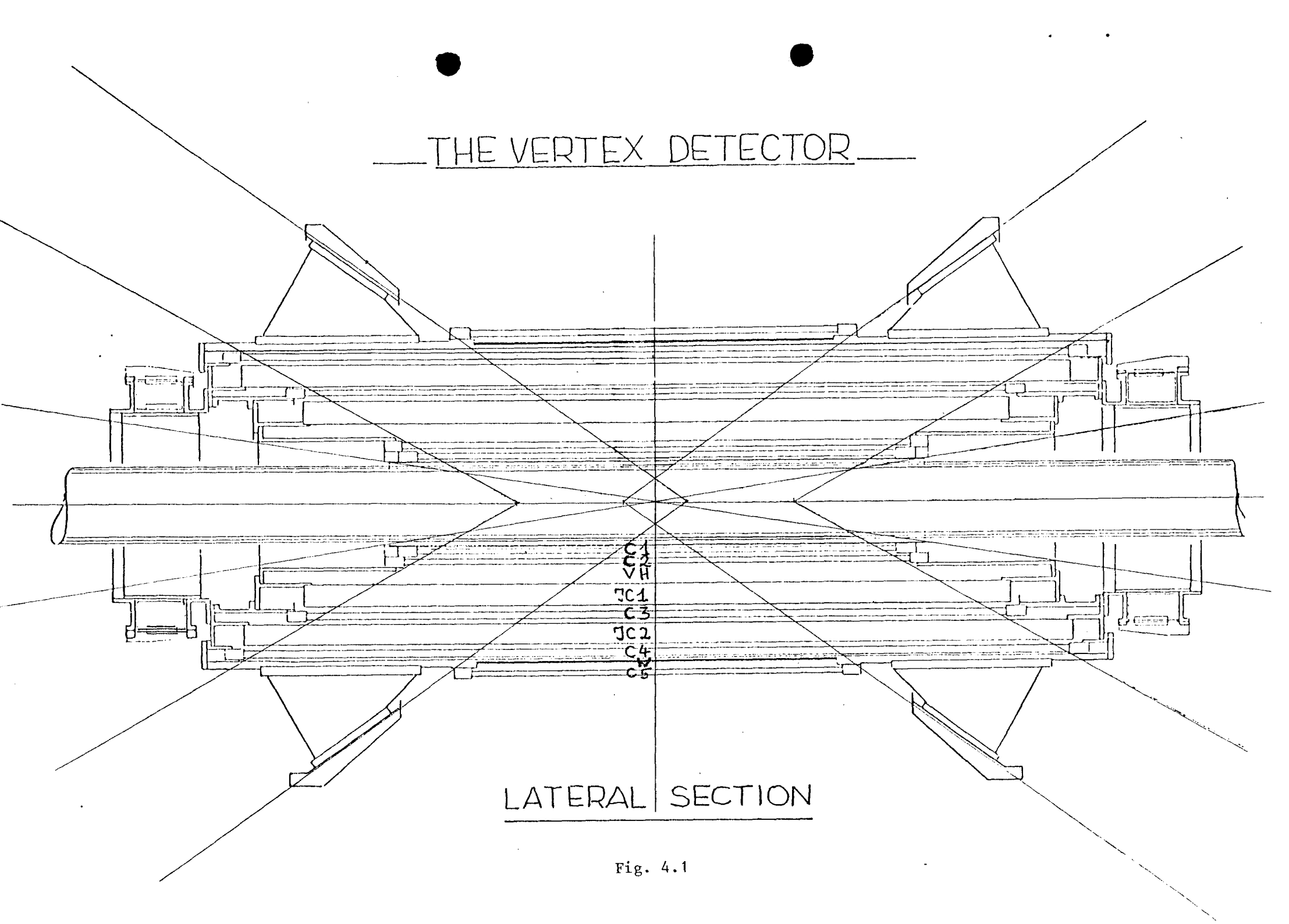

Fig. 4.1

The strip width is 3 mm and the spacing between strips is 1 mm. The Rohacell foils are smoothed to a precision of ± 0.1 mm to their designed thickness, then rolled in a helix form on a moulded cylinder. Together with the glue (Araldite) between the Kapton foils and the Rohacell this gives a rigid, nevertheless light cylinder, which does not need external reinforcement. Between 2 of such cylinders with strips helical at ∿ ±45° the proportional wires out of gold plated W - Rh of 20 µ (wire spacing of 2 mm) are soldered parallel to the cylinder axis keeping a gap of 4 mm with respect to the strips.

The HT of ∿ 2 500 V is brought to every 16 th wire and then distributed to the others. The strips are kept at ground potential by the amplifier. Tests of chambers C1 to C3 gave a gain of ∿ 10^5 with a variation of about a factor 2 over the whole chamber which shows the quality of the construction technique.

The gas mixture used will be magic gas (Argon - Isobutane - Freon : 79.8 % / 20 % / 0.2 %) enriched with 1 % Freon. For the C1 to C4 there are in total 2102 wire and 1680 strips. The radiation lenght for C1 and C2 is 2.2 ‰, for C3, C4, C5 2.5 ‰.

4.1.2 - Electronic of the strip chambers

The wire signals and the strip signals are amplified with the same fast, low noise current preamplifier developped in ORSAY (LAL-RT-79/3, Juin 1979). After a 85 m twisted pair cable all signals are amplified in Line-Receiver modules which eliminate the common mode noise. The wire signals are then read by a memory unit built in ORSAY. The strip signals are digitized by a 48 channel ADC type 2282 E of LECROY.

4.2.1 - Mechanics of the jet chambers JC1, JC2

A jet chamber consists of the 24 drift cells on a self supporting cylinder; each cell is separated by walls and covered by it's own ceiling. The self supporting cylinder is made by using the same sandwich technique already described for the strip chambers. To have more rigidity, Rohacell foils of 1.5 mm are used. The 24 walls are made of printed boards of 300 µ (260 µ fiber glass, 20 µ Cu each side). The ceiling for each drift cell is also made of a Rohacell, Kapton sandwich. Each end of a chamber is termined by a fiber glass cylinder to give the support for the sense and potential wires. One driftcell is completely surrounded by field shaping strips including the end plates transverse to a driftcell, to guarantee a uniform

electric field over the full lenght of a driftcell. By the construction method each cell is kept independent to allow for individual handling (i.e repair). Each cell has 6 sense wires of 25μ NiCr and 7 potential wires of 50μ W-Rh with 4 mm gap between two wires (see graph below). The sense wires are staggered by 400μ to minimize the left/ right ambiguities.

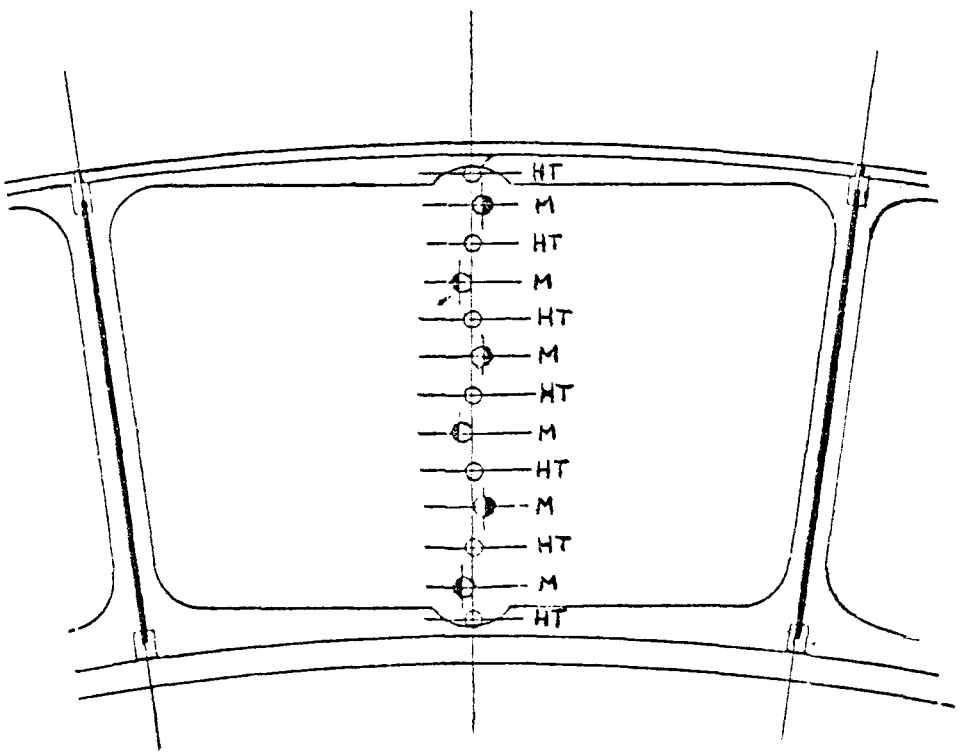

The sense wires are grounded, the potential wires kept at ∿2300 V; the field shaping strips have a maximum voltage of 4000 V for JC1 and 5200 V for JC2. The voltage are graduated to obtain an electric field of ∿ 1000 V/cm. The track resolution measured with a prototype was 220 μ in the (r, Ø) plane and 7 mm in the (r,z) plane. The two particle resolution will be of about 100 ns. The gas mixture used will be Argon-Ethane (50% / 50%), JC1 and JC2 have altogether 288 sense wires.

4.2.2 - Electronics

For the readout of the sense wires the charge division method is used. At both ends of a wire the signal is amplified with the same type of preamplifier used for

the strip chambers. After a 20 m twisted pair cable the charges measured at both ends of a wire are filtered, fanned, added and discriminated to define the drift-time signal. The 2 charge signals (charge $_{left}$, charge $_{right}$) are sent over a 85 m twisted pair cable to a charge integrator unit which includes a Line-Receiver and linear filter to eliminate the common mode noise and reduce the tails from the cable before they are sent to an ADC. The timing signal is sent over a 65 m twisted pair cable to a TDC. The drifttime signal is used to define the gate for the integrator. The difference in cable length is necessary to allow for correct timing between the drifttime digitization and the charge integration. The TDC, the integrator and the ADC have multihit capability of up to 8 hits. The TDC and the ADC information are stored into a memory in the order charge$_{left}$, charge$_{right}$, drifttime, so that the correlation between the charges and the time is kept. The memory is then read by CAMAC. All units are made in ORSAY.

4.3 - Scintillator hodoscope

The scintillator hodoscope is made of 24 strips of NE 110 (a strip is 4 cm wide, 0.5 cm thick and 120 cm long). A phototube (type XP 1910 from Radio Technique) at each end collects the light. The signal from each end is sent over a 85 m coaxial cable to a Multiconverter unit. This unit contains discrimination, charge measuremen time measurement, meantimer and veto.

4.4 - 5th MWPC

A 5th MWPC with 1.5 radiation lenghts of Tungsten in front is used to have a better localisation of the beginning of the electromagnetic shower. This chamber is mechanically constructed in the same way as the 4 other MWPC's. The differences are :

a) The wirespacing is 4 mm
b) The wires are connected together in pairs with charge division readout at each end of a pair.
c) For the wires 25 µ NiCr or 20 µ Inox will be used which will allow for charge division.
d) The voltage will be lowered by ∿ 200 V of its nominal value. This avoids additional support for the wires in between the cylinders and allows to use the same electronic chain as for the other chambers (avoids saturation).

On the average there will be always 2 wires hit, because the enveloppe of the electromagnetic shower will be of the order of 1 cm (motivation for increasing the

wire spacing and connect them together). Because the strips readout is kept the same as before, the precision of the localisation of the shower centroid should be the same as for the others chambers (σ= 200 μ). The charge division measurement will help to solve ambiguities.

5 - F/B DRIFT CHAMBERS

The drift chambers to be used in the forward/backward detector of the UA2 experiment are built by groups from the Universities of Copenhagen and Pavia.

The trapezodial shaped chambers are situated in a ring just outside the toroid-magnet in such a way that the frames are in the shadow of the magnet coils as seen from the center of the overall detector. Each magnet has twelve sets of coils leading to twelve sets of chambers. A set of chambers consist of three chambers in different sizes. Every chamber has steel frames for mechanical rigidity. The frames which hold the wires are made from vetronite. The wires are soldered on printed circuit boards glued onto the vetronite frames. Each chamber has three detector planes with the wires parallel, and $\pm 7^{\circ}$, to the magnetic field. The small angles are chosen mainly to optimize the momentum resolution as the direction at the vertex is determined in the vertex detector proper.

Each chamber has the wires arranged in the order 7°, 0, and -7°. The chambers, which are conventional drift chambers have a cell width of ± 5 cm. The number of cells are for the small chamber 9, 10, 9, for the medium chamber 10, 11, 10, and finally for the large chambers 12, 12, 12, respectively. The transverse dimension of the cell, as determined by the width of the vetronite frames, is 10 mm. The field shaping wires are spaced 5 mm. This causes some leakage of the field from one plane to the next. To avoid this, an aluminized mylar foil is inserted between the planes. A voltage of half the maximum field voltage is applied to this plane. The field wires are Cu-Be wires with a diameter of 100 m and a tension of 130 g and the sense wires are goldplated W-U wires of 20 m with a tension of 60 g. On the prototype to be discussed later we used 100 g and 50 g respectively.

The voltage on the individual fieldwires is obtained using a simpel linear voltage divider. A given voltage is fed to all the cells via a bus on a double sided printed circuit board. To test the correct functioning of the electronics a testpulse can be injected into the sensewires again using a bus. The preamplifiers have a risetime of 6 ns and a slewing of 6 ns.

A set of three chambers give 95 signals. We have chosen to feed these signals to 6 cards with 16 preamplifiers on each, i.e. 96 in total per set. This brings the total of signalwires to 2 x 12 x 96 = 2304.

The aluminized nylar foils are 20 μm thick with a 8 μm layer of Al on each side.

A prototype of the smallest size chamber was built and operated under various conditions. The chamber which is 130 cm long weighs about 180 kg. The construction and assembly technique which is common to all chambers appears to be satisfactory. It involves an enlarged version of the CERN wireing machine, the use of combes and soldering and assembly tables. The prototype was soldered by hand, while the real production will be done by an automatic soldering machine to reduce the manpower requirement.

The chamber was operated with various gas mixtures of argon and ethane. For the measurement given in the figures a mixture of 70% argon and 30% ethane was used.

A picture of the chamber is shown in fig. 1. The output circuit is shown in fig. 2. Fig. 3 shows typical output signals on a 50 load. The signals have a size of 5-15 mV and a risetime of the order 30 ns.

The first test were done using cosmic rays and a β -source.

An example of an efficiency measurement is shown in fig. 4. The absolute normalization is given by a small scintillation counter in the center of the chamber. The plateau is reached already at a positive voltage on 1.1 KV on the sense wire. The negative voltage was kept on 3 KV and the threshold was as low as 0.33 mV.

The saturation properties of the drift velocity was studied with a collimated source and a system of downstream collimators and two counters in coincidence. The whole assembly was mounted on a precision transport system which can be moved orthogonally to the wire direction.

The time delay between the scintillator coincidence (intrinsic resolution $\sim$ 250 ps) and the chamber pulse was measured as function of position. A gaussian fit to a selected portion of the spectrum gives the peak position to about 50 μm. The dependence of the drift velocity on negative voltage is shown in fig. 5. Around HV^{-} = 4 KV velocity saturation appears, at a value of $V \sim 51$ mm/μs, calculated from maximum and minimum time difference.

6 - F/B MULTITUBE PROPORTIONAL CHAMBERS

A device for the localization of electromagnetic showers will be installed in front of the forward-backward (F/B) calorimeters, in order to reduce in the search for leptonic $W^{\pm}$-and Z^{o}-decays the background, which will mainly be due to the overlap of a neutral hadron induced electromagnetic shower with a charged hadron within the same calorimeter cell. The required shower localization was estimated to about 1 cm and, therefore, may be realized by means of multitube proportional chambers (MTPC). The advantages of this solution are reliability (homogenous gain), simplicity and also absorption of low energetic shower components in the tube walls.

Description of the chambers

One MTPC consists of two coordinate planes: The coordinate axes include an angle of 77^{o}. The whole chamber geometry is given by the "umbrella" structure of the F/B detector, as shown in Fig. 6.1.

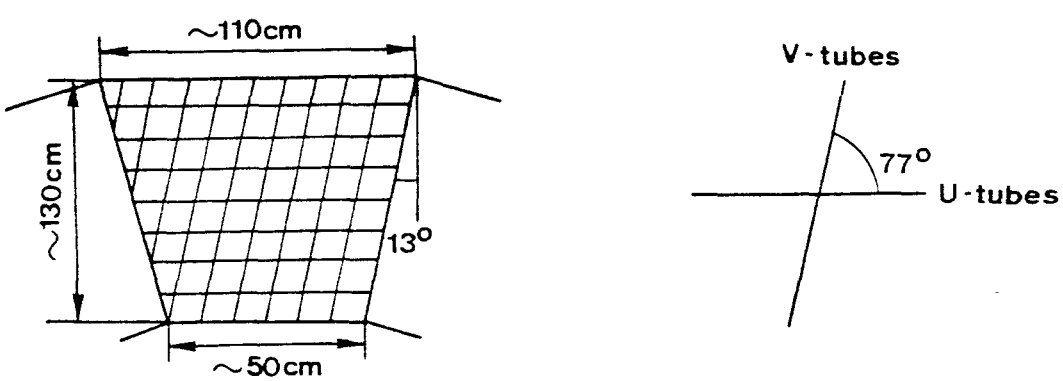

Fig. 6.1: Chamber geometry

Each plane is made up of a double layer of brass tubes with an outer diameter of 20 mm and a wall thickness of 0.3 mm

(Fig. 6.2)[1]. The tube anode (sense wire) is a 30 µm diameter gold plated tungsten wire.

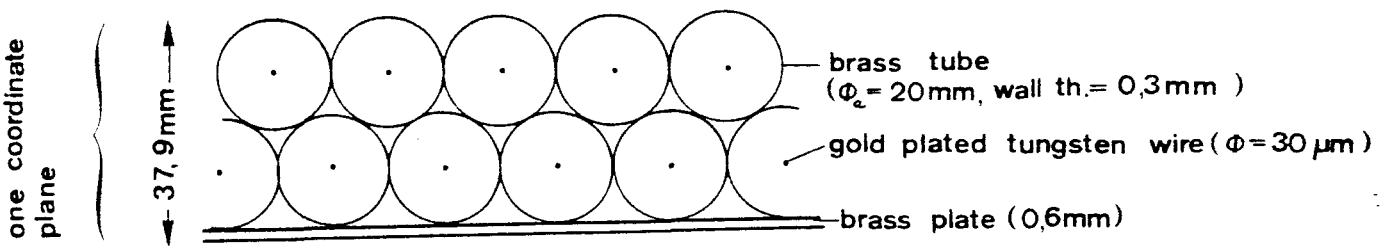

Fig. 6.2: Tube geometry and staggering

To generate electromagnetic showers a converter, consisting of a 5 mm thick steel and a 6 mm thick lead plate (totally about 1.4 radiation lengths), is placed in front of each chamber.

The chamber gas, a mixture of 80 % argon and 20 % CO_2, will be applied at a flow of about 5 ℓ/h.

Electronics

Fig. 6.3 shows a block diagram of the chamber electronics and the cabling to the counting house. The part of the electronics within the dotted square is situated in a box at the outer edge of each chamber. The sense wires are connceted to this box by means of flat cables.

The preamplifiers, discriminators and delay circuits are realized with standard ICs: 1 µA733, 1/4 MC10125, 1/2 LS221 and 1/2 LS74 are needed per channel. An 8 bit shift register LS165 constitutes the memory for the eight channels per printed circuit board, and 29 such circuits per chamber are connected in

---

1) B. Neumann, Diplomarbeit der Universität Hamburg (1978), DESY F33-79/01.

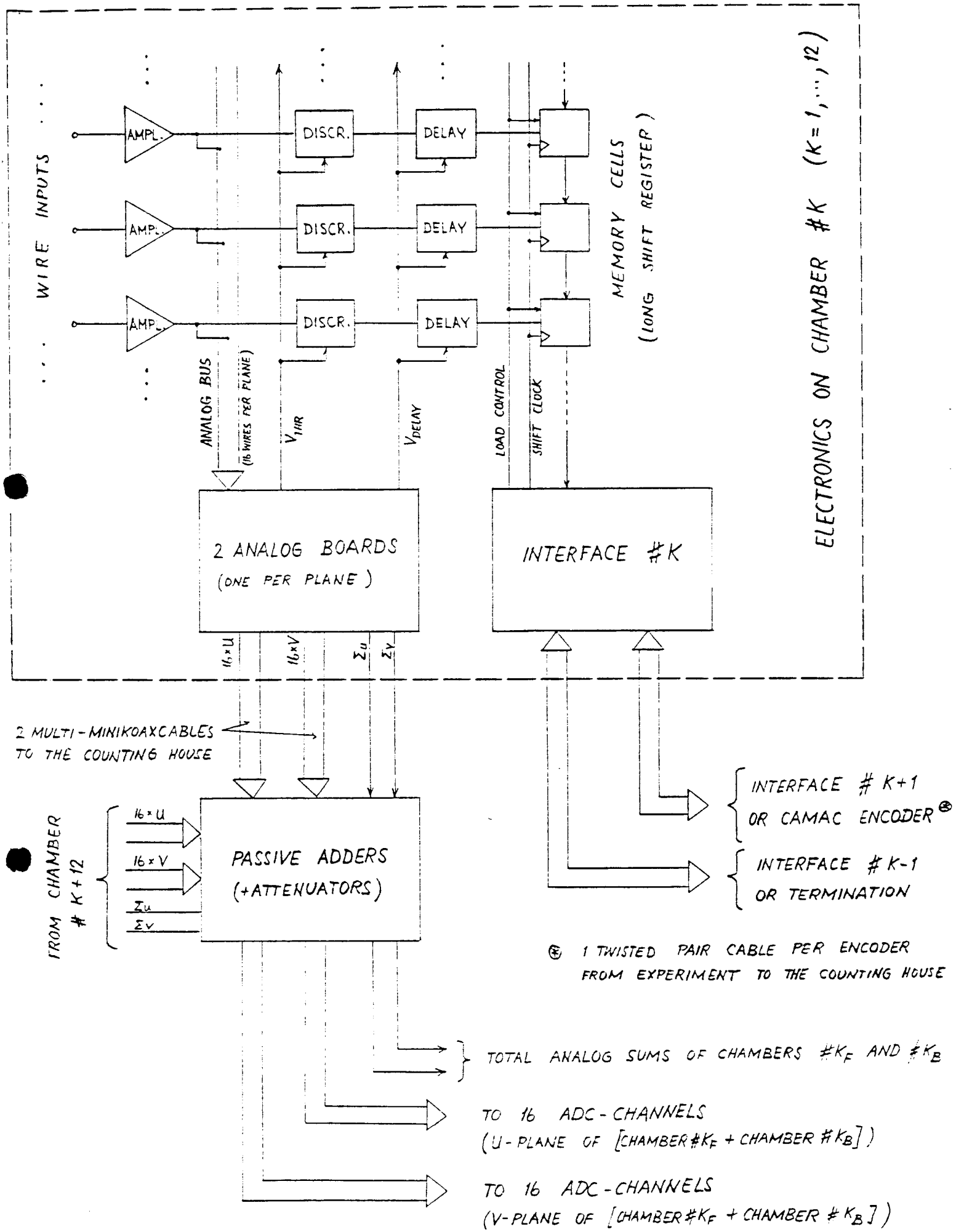

Fig. 6.3: Block diagram of the MTPC electronics

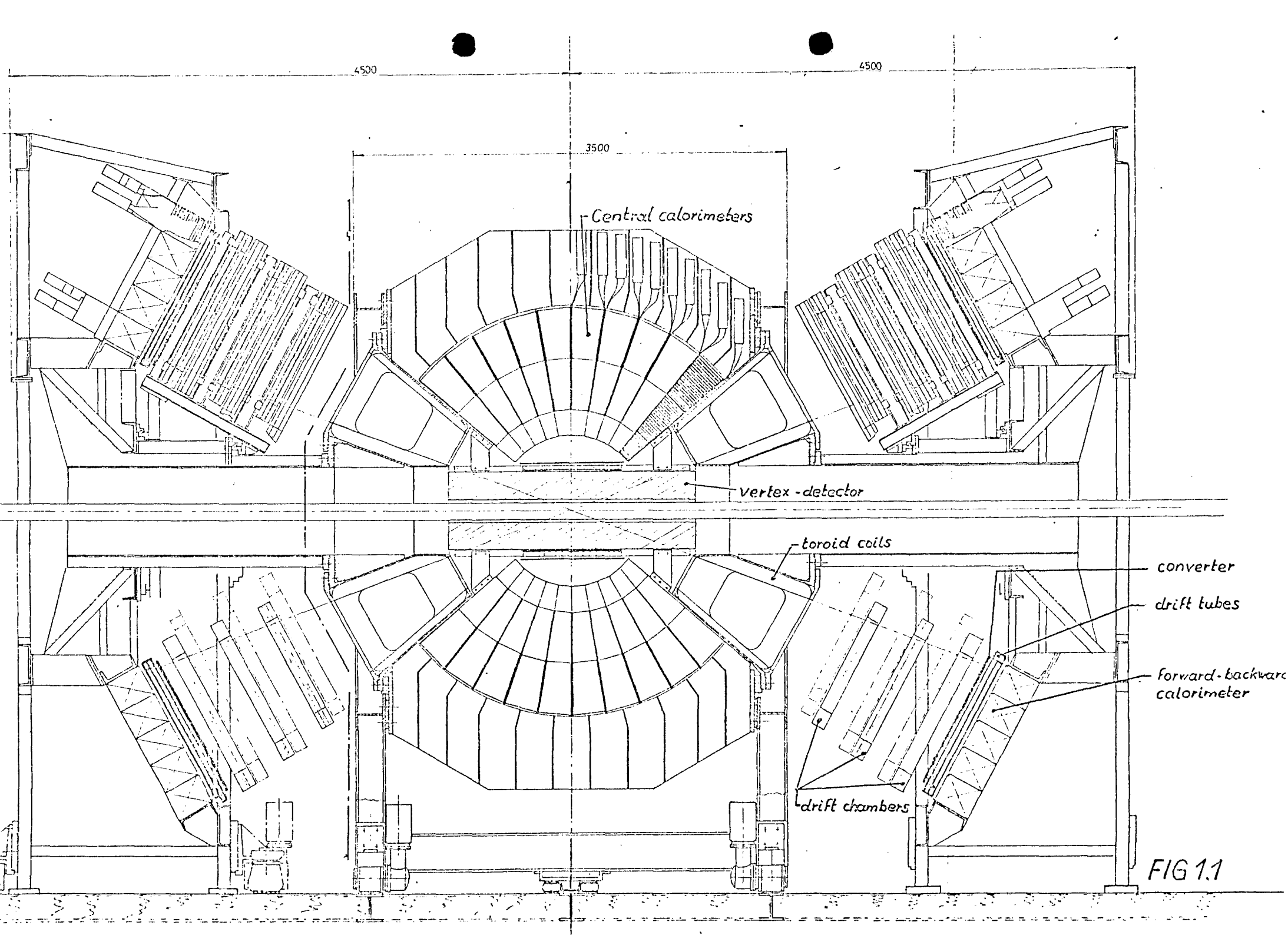
4500
4500
3500
Central calorimeters
vertex - detector
toroid coils
converter
drift tubes
forward - backward
calorimeter
drift chambers

FIG 1.1

series forming a 232 bit long shift register. The serial read-out of these long shift registers is achieved by means of the pulse-width modulation method [2].

For economical reasons only a limited number (384) of ADC-channels are used to record the charge on the sense wires. Adding the analog signals of the forward and the backward chambers located at the same azimuth, 32 ADC-channels are available per chamber. The necessary grouping of the 226 signals of each chamber is done in the following way: A current-like signal is fed from each preamplifier output into the analog bus. This bus consists of 16 signal lines ($i = 0$ to 15) per plane which transmit the analog sum of 6 to 8 wires: The signals of the wires $n = i + k \cdot 16$ ($k = 0$ to 7, $n \leq 125$ or 101, respectively) are added up on these lines. The analog sum signals are amplified on the two "analog boards" for the U- and for the V-plane, respectively.

Performance

a) Tests with small tube setup:

To investigate the performance of the proposed MTPC system with respect to the detection and localization of electromagnetic showers and hadron rejection, as well as to fix some parameters (converter thickness, operational high voltage, discrimination level), a small tube setup has been exposed to an electron/hadron beam in the momentum range between 20 and 60 GeV/c. The arrangement of the tubes (two coordinate planes, each consisting of 11 tubes staggered in two layers) corresponded to that of the real chambers (Fig. 6.1, 6.2). A typical efficiency behaviour for electrons and hadrons, obtained at 1650 V, with a converter of 1.9 radiation lengths and with a discrimination level, corresponding to about eight

---

[2] A. Beer, F. Bourgeois, A. Corre and G. Critin, yellow report CERN 78-14 (1978).

times minimum ionization, is shown in Fig. 6.4. For this case, the uncertainty in the localization of electromagnetic showers was found to be about ± 5 mm.

b) Tests with prototype chamber:

With the prototype chamber only a few test measurements have been made up to now, mainly to investigate the behaviour of the gain with respect to the amount of primary ionization in the tubes. For this we use the following three reference peaks: The cosmic ray peak and two X-ray photopeaks, one originating from a 27.3 keV Te K-X-ray line (produced by a ^{125}I (EC) source), the other from a 8.6 keV K-X-ray line (induced by the 27.3 keV radiation in the tube material Cu/Zn). Fig. 6.5 shows the three peaks as obtained at the operational high voltage (1650 V).
By means of these peaks, it is possible to scan the gain/ionization behaviour of the tubes over a wide range by variing the high tension to simulate different primary ionizations. The result is plotted in Fig. 6.6.

A summary of the essential tube data and the parameters for a proper operation in the UA2-experiment are given in the following table.

Table 6.1: Tube data and operational parameters

outer tube diameter	20 mm
inner tube diameter	19.4 mm
sense wire diameter	30 µm
gas mixture	80 % Ar / 20 % CO_2
gas flow	~ 5 ℓ/h
operational high voltage	~ 1650 V
gas amplification	~ 10^4

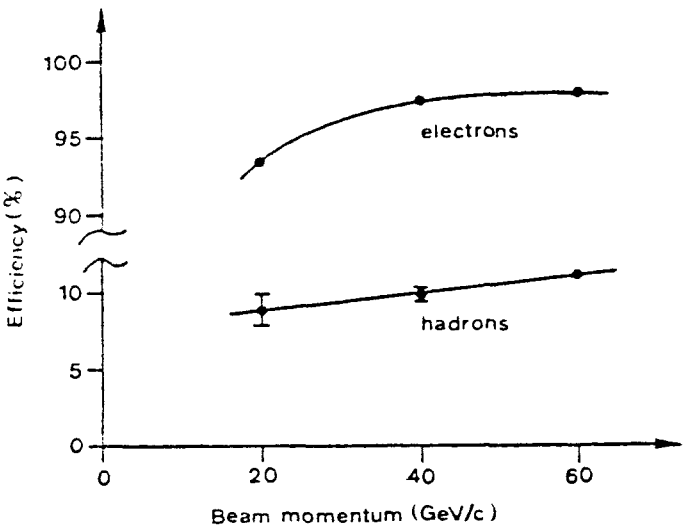

Fig. 6.4: Electron and hadron efficiencies at a typical discr. level

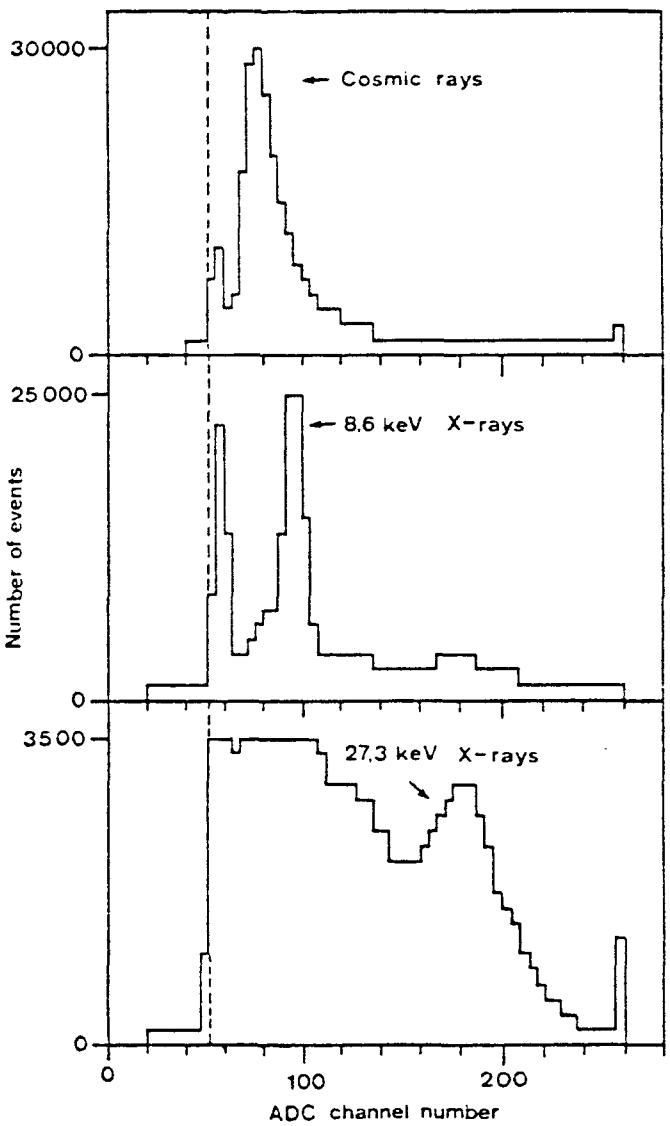

Fig. 6.5: Reference peaks

Fig. 6.6: Linearity behaviour of response

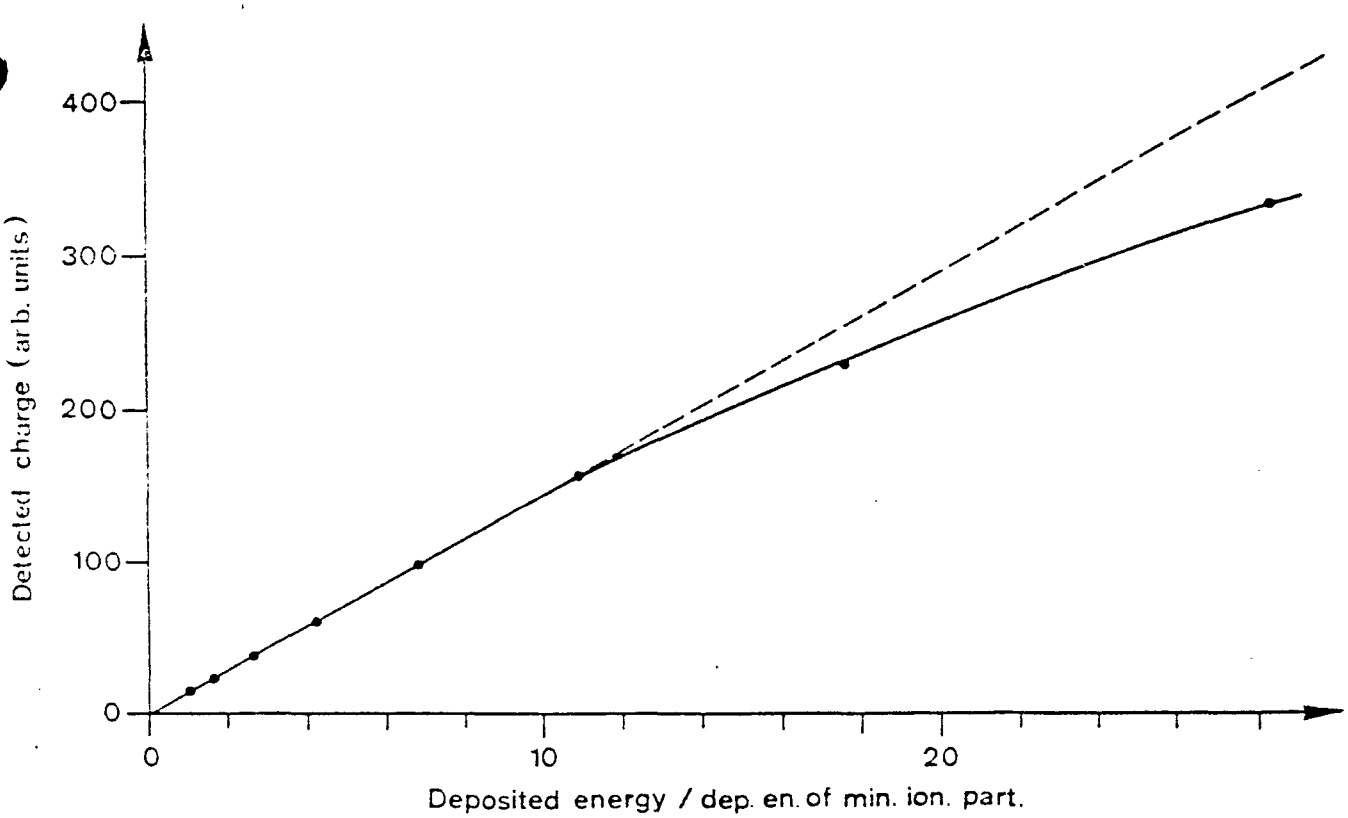

7 - THE FORWARD/BACKWARD CALORIMETER

Description. Each of the two forward-backward calorimeters is composed of 12 sectors covering 30° in azimuth and 20° in polar angle (Fig. 7.1). Each sector consists of 10 cells having the same $\Delta\theta$, $\Delta\phi$ coverage. A cell is subdivided in 4 mm altustip scintillator plates sandwiched between 4 mm lead plates and is assembled in two stacks, the first 24 radiation lengths thick and the second 6. The light produced in each scintillator stack is collected by two BBQ wave length shifters, and viewed by two RTC 2008 photomultipliers. In this experiment, we need to measure energies between 0.2 GeV and 200 GeV and, therefore, the photomultiplier signal has to be analysed in two 12-bit ADC's, the second ADC receiving the signal after an amplification of 15.

All the calorimeters are equipped with a calibration system identical to the one used in the central calorimeter.

Performance of a test module. 1) Electrons. A 1:1 scale module prototype was tested in an electron beam of the CERN SPS with beam energies of 10, 20, 40 and 80 GeV. The calorimeter response is shown on Fig. 7.2 where the signals of the two BBQ bars of a module were linearly added. The response is linear to better than 1%. The resolution can be parametrized by $\sigma_E/E = 15 \times 10^{-2}/\sqrt{E}$.

The response of the calorimeter as a function of the beam impact point has been studied. Fig. 7.3 shows the response of each phototube as a function of the position in the cell. The pulse height of each phototube is changing by a factor of 4 between the two edges but the sum of the signals of the two phototubes is increasing by only 40% between the center and the edges. In the experiment, however, the impact point of the electron will be known to a precision of better than 5 mm.

2) Muons and Hadrons. In order to check the calibration system it is important to know the response to minimum ionizing particles. This is shown for the front and the back part in Fig. 7.4. The full thickness of the calorimeter represents 1 collision length and thus cannot fully contain the shower induced by a strongly interacting particle. However, when

a hadron interacts in the first part of the calorimeter it may deposit a large fraction of its energy. For an electron, the shower is almost fully contained in the first cell (24 radiation lengths), whereas a hadronic shower extends to the back cell. Therefore, a good rejection against hadrons can be obtained by requiring that less than 3% of the total energy is in the back compartment. The efficiency for electrons is better than 99%.

FIGURE CAPTIONS

Fig. 1.1 Cross-section along beam line through UA2-detector.

Fig. 1.2 1:10 scale model of detector (back detector, symmetric to forward detector, not shown).
A. Symmetric configuration, with toroid coils and forward detector recessed.
B. Wedge configuration.

Fig. 2.1 Details of individual cell of central calorimeter.

Fig. 2.2 Energy resolution of central calorimeter as a function of energy for electrons and hadrons.

Fig. 2.3 Response of individual photomultipliers in third-largest electromagnetic cell in central calorimeter to 40 GeV electrons, as a function of impact point.

Fig. 3.1 Cross-section perpendicular to the beam through detector in the "wedge" configuration.

Fig. 5.1 Prototype chamber.

Fig. 5.2 Output circuitry.

Fig. 5.3 Output pulse on a 50Ω load. Vertical scale 10 mV/cm, horizontal scale 50 ns/cm.

Fig. 5.4 Absolute efficiency curve as a function of the positive sense wire voltage for the median plane.

Fig. 5.5 Dependence of the drift velocity on the negative voltage applied to the cathode wire system.

Fig. 7.1 Forward-backward calorimeter sector.

Fig. 7.2 Calorimeter response to 10, 20, 40 and 80 GeV electrons.

Fig. 7.3 Response to electrons as a function of position in the cell. The signals are normalized to 1 at the center of the cell.

Fig. 7.4 F/B calorimeter response to minimum ionizing particles in the front and the back part. The signal in the front part has been amplified by a factor of 10.

Fig. 7.5 Calorimeter response to 80 GeV hadrons and electrons. The peak at 80 GeV corresponds to electrons, while the large structure between 0 and the electron peak corresponds to hadrons having interacted in the calorimeter.

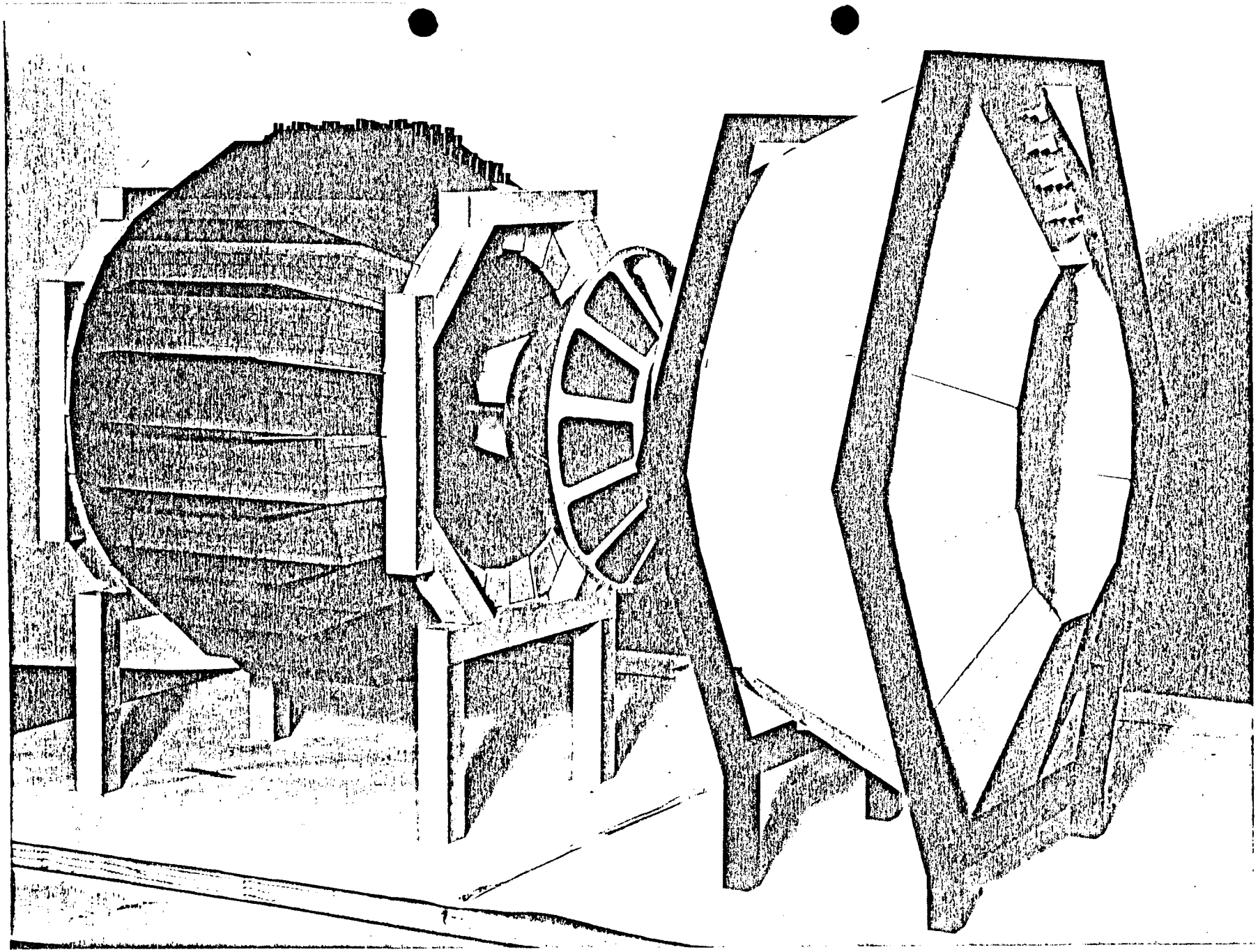

FIG 1.2 A

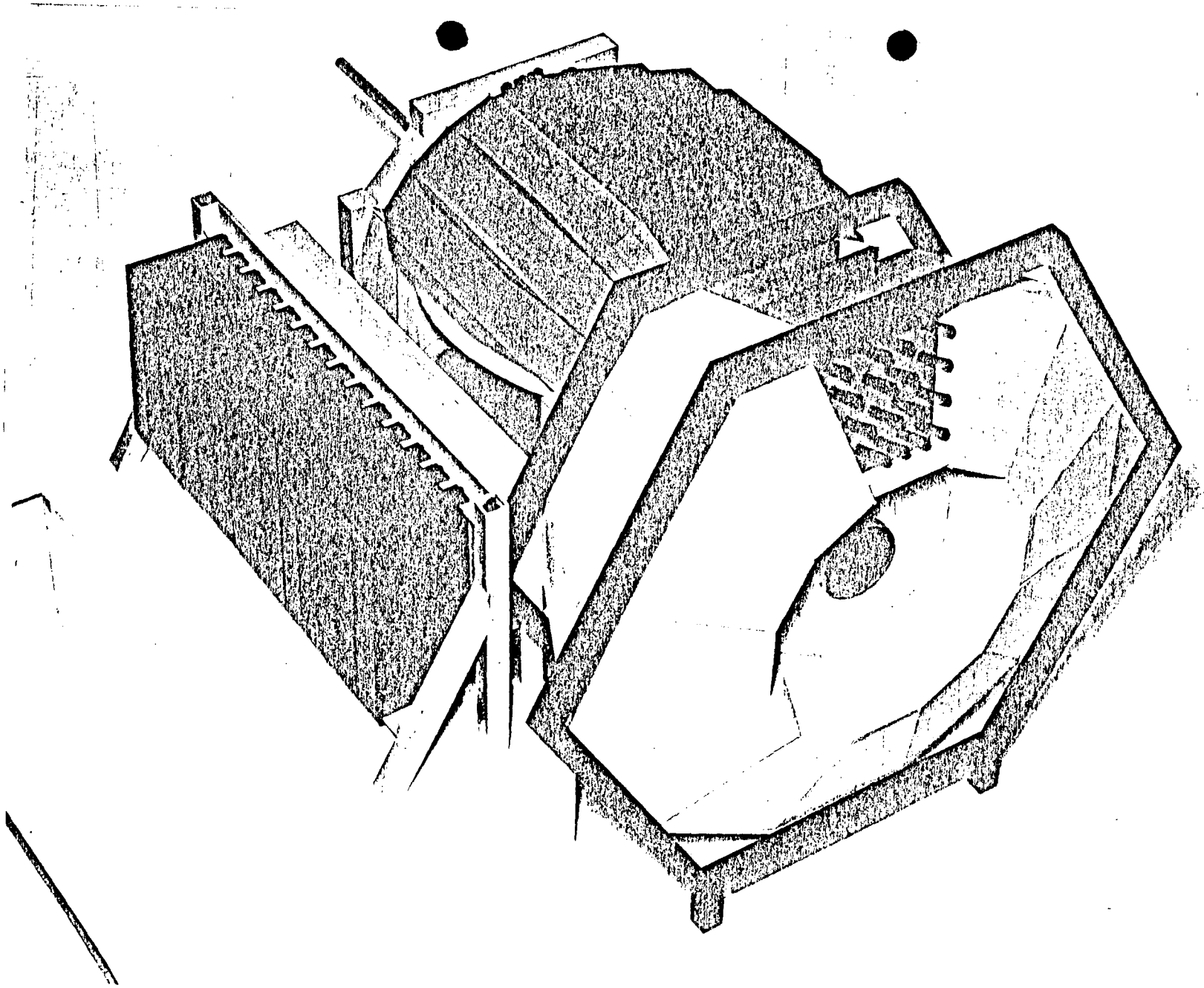

FIG 1.2. B

CENTRAL CALORIMETER CELL

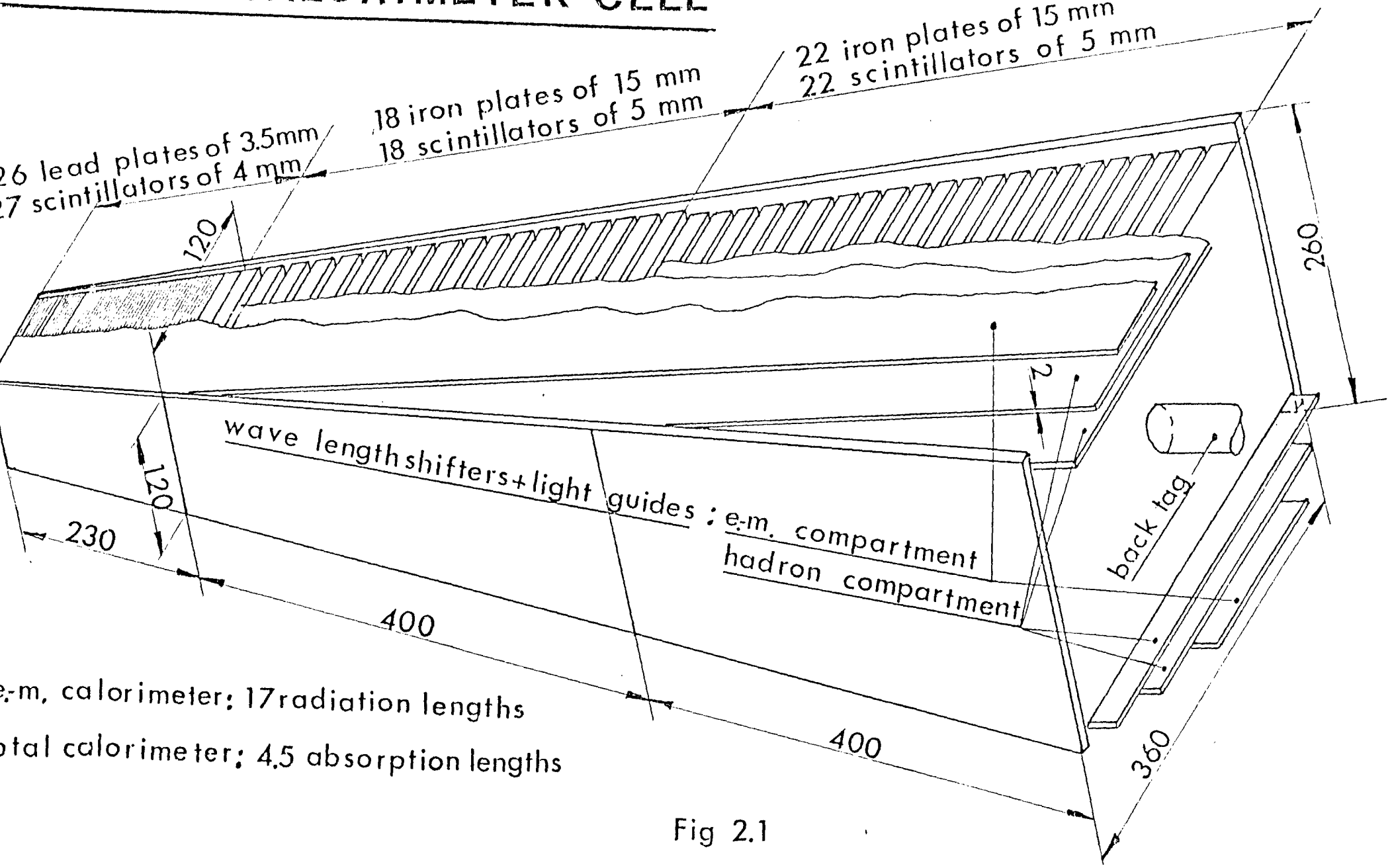

e-m, calorimeter: 17 radiation lengths

total calorimeter: 4.5 absorption lengths

Fig 2.1

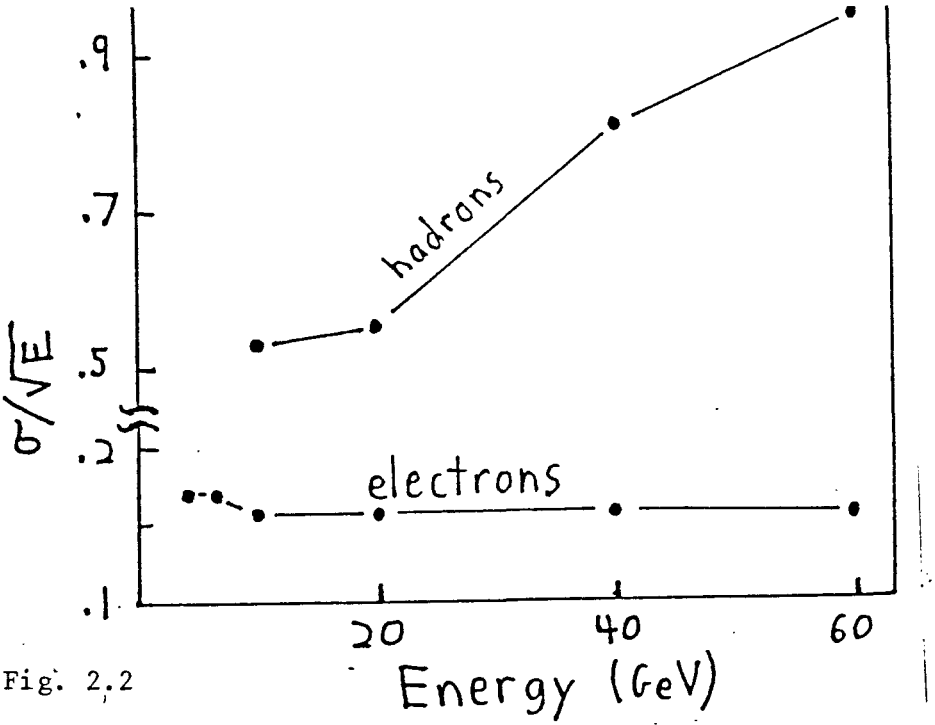
.9
.7
.5
.2
.1
σ/√E
hadrons
electrons
20
40
60
Energy (GeV)

Fig. 2.2

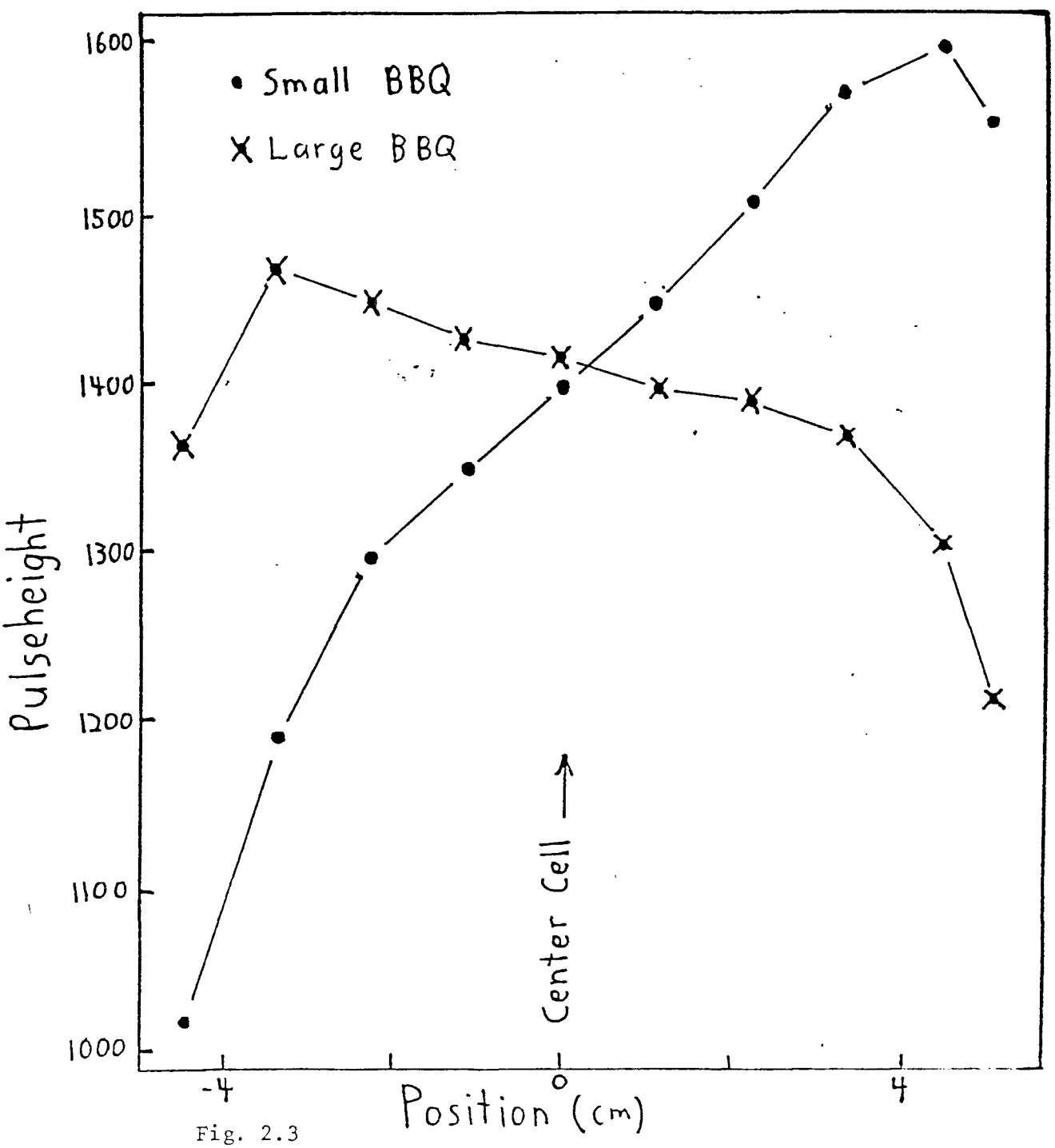
1600
1500
1400
1300
1200
1100
1000
Small BBQ
Large BBQ
Pulseheight
Center Cell
-4
0
4
Position (cm)

Fig. 2.3

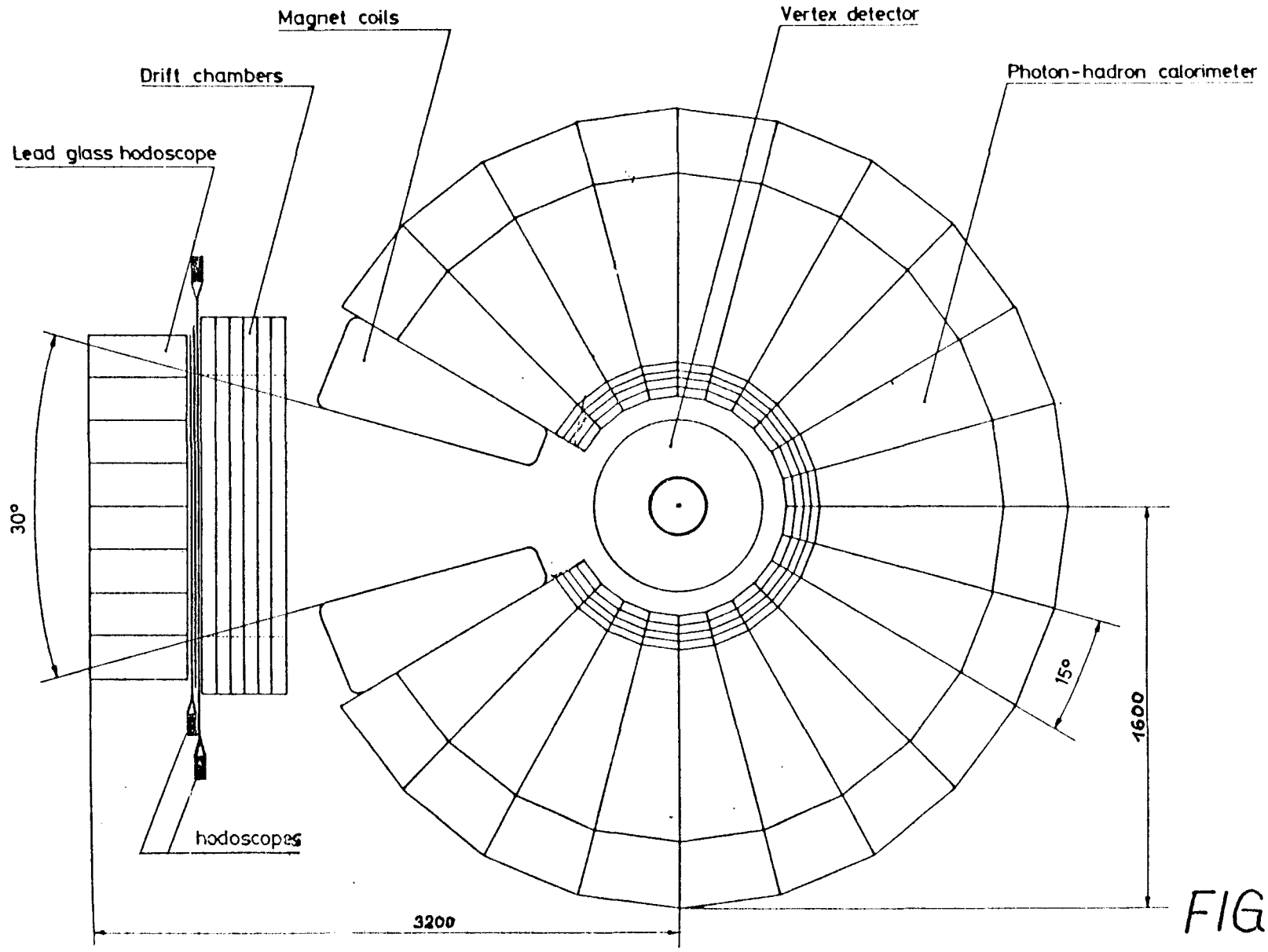
Magnet coils
Vertex detector
Drift chambers
Photon-hadron calorimeter
Lead glass hodoscope
30°
15°
1600
hodoscopes
3200

FIG 3.1

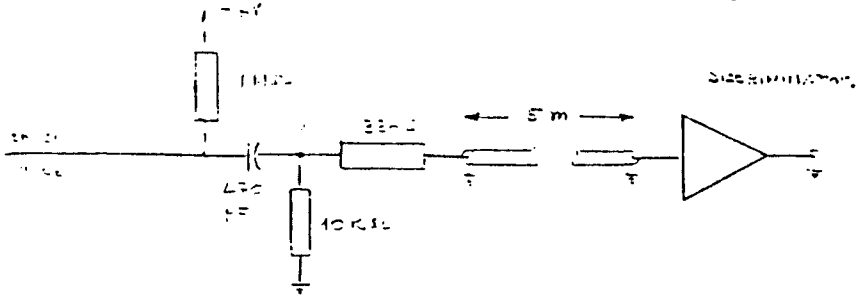

Fig.5.2 Output circuity

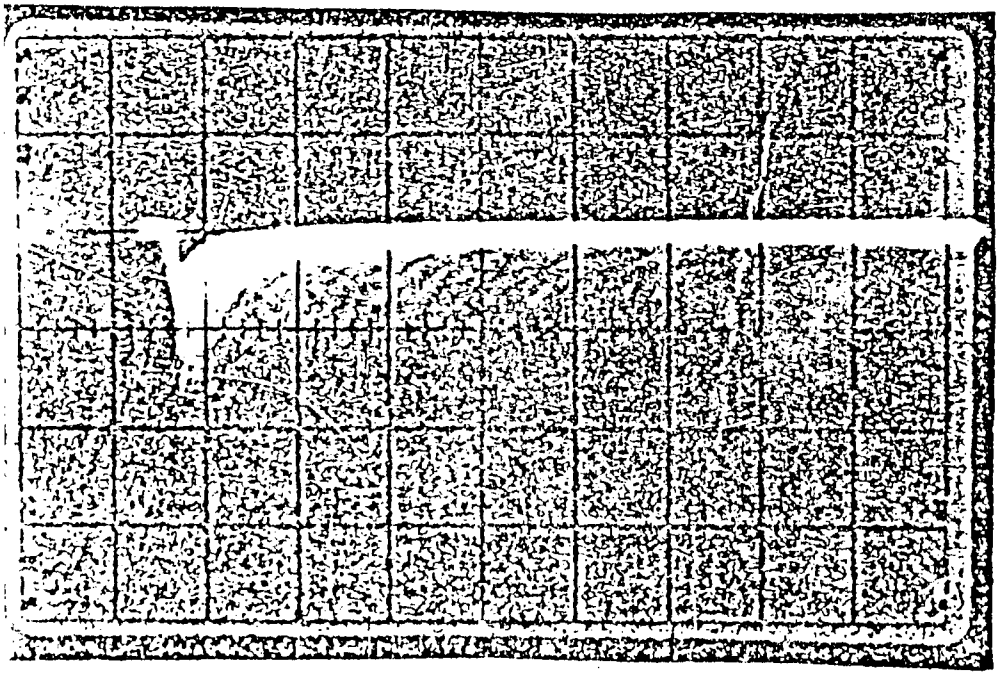

Fig.5.3 Output pulses on a 50 Ω load vertical scale 10 mV/cm horizontal scale 50 ns/cm

THE VERTEX DETECTOR

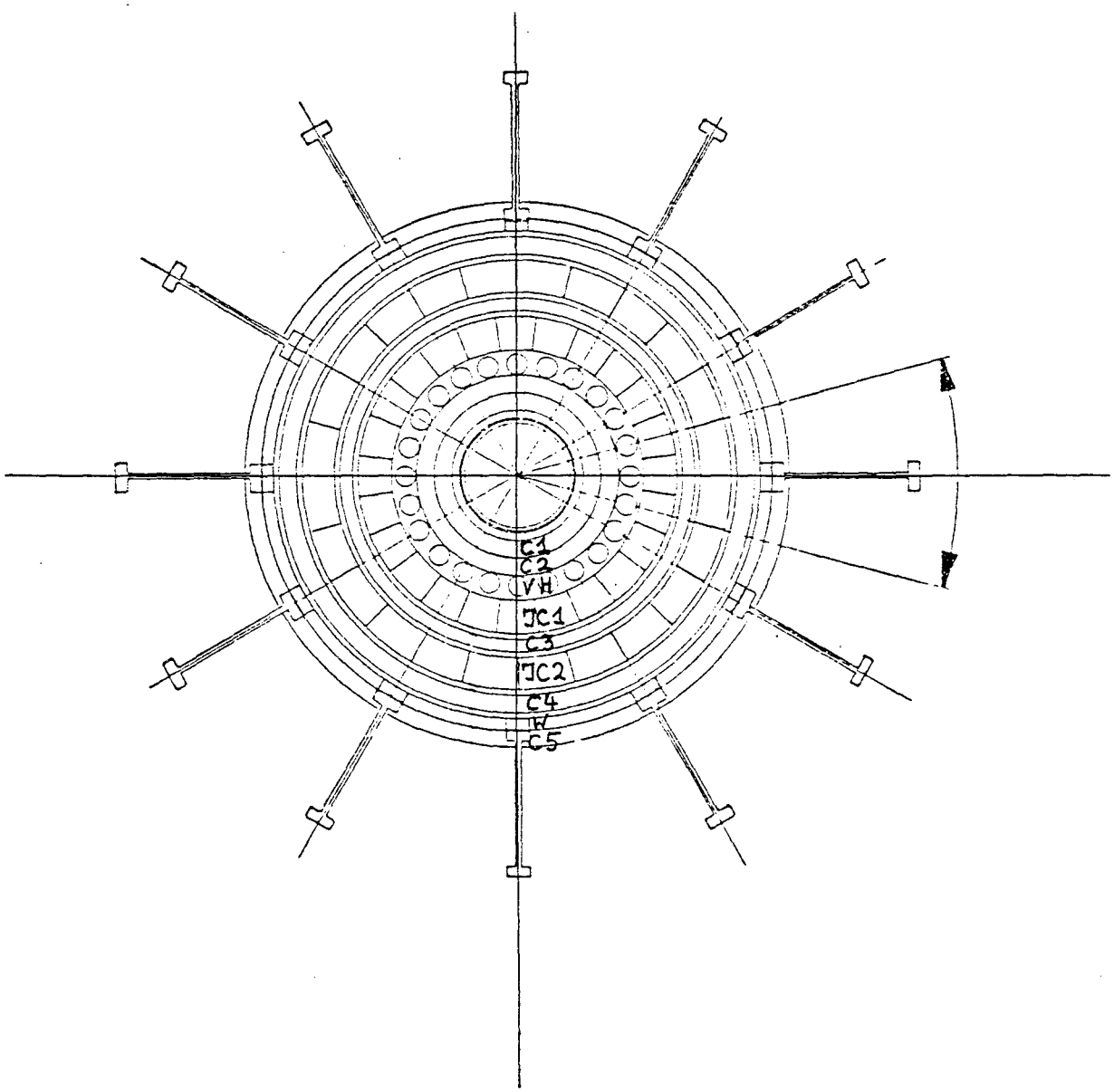

VERTICAL SECTION

Fig. 4.2

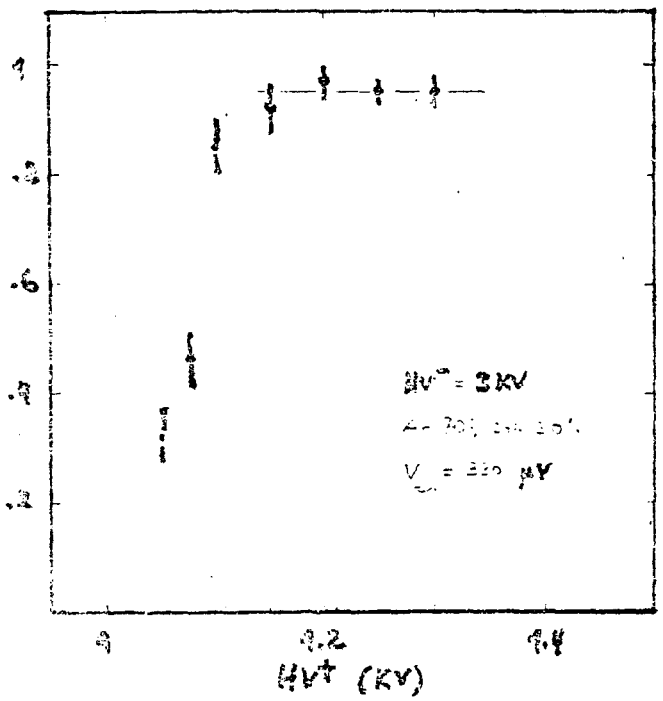

Fig. 4 Absolute efficiency curve as a function of the positive sense wire voltage for the medium plane.

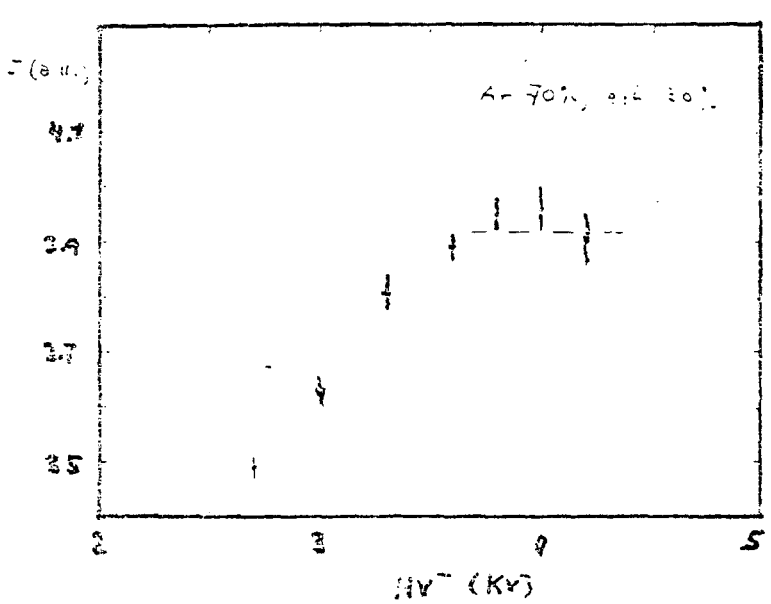

Fig. 5.5 Dependence of the drift velocity on the negative voltage applied to the cathode wire system.

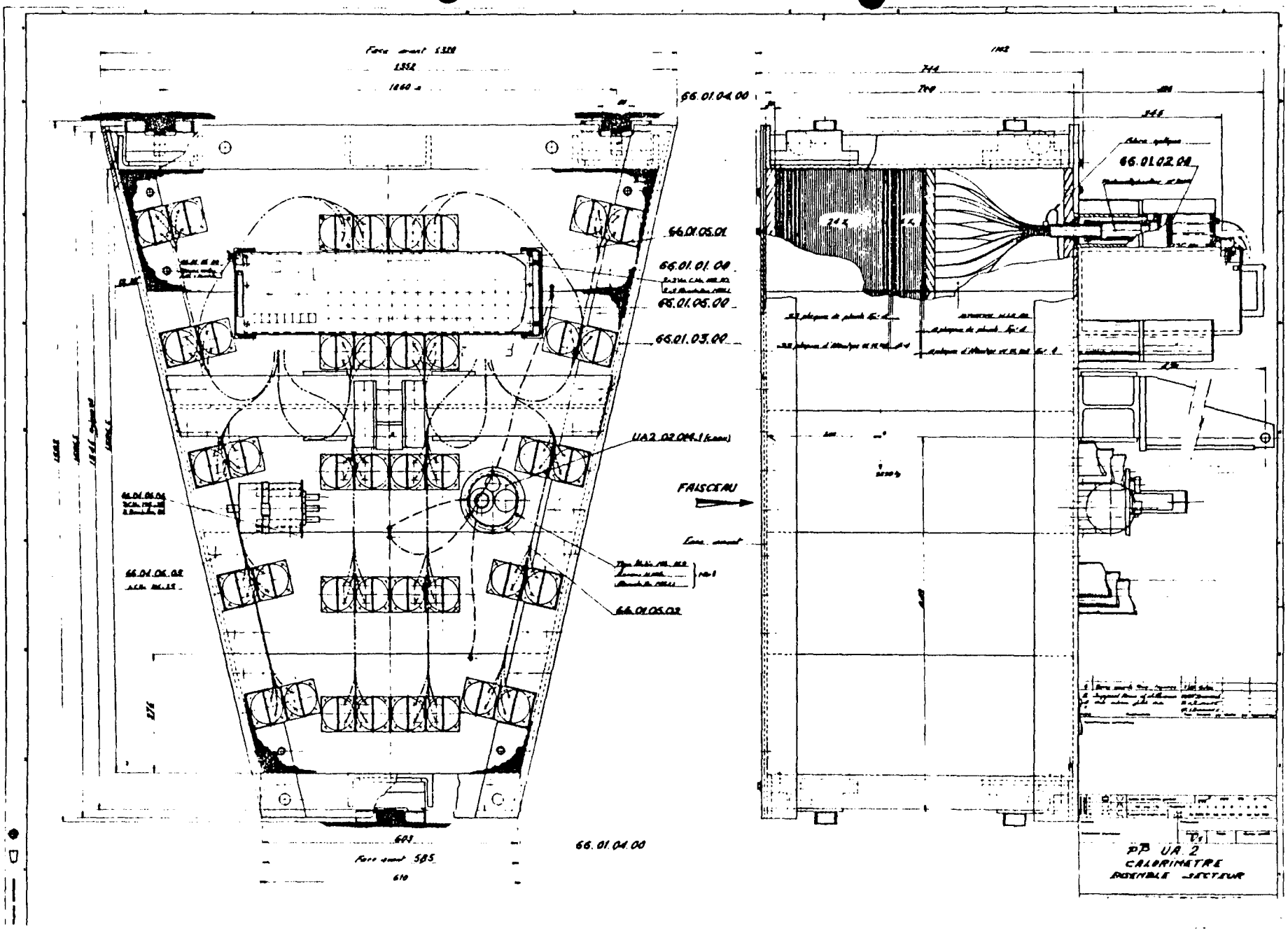
66.01.04.00
66.01.05.01
66.01.01.00
66.01.05.00
66.01.03.00
FAISCEAU
66.01.05.02
66.01.02.00
66.01.04.00
PB UA 2
CALORIMETRE
ENSEMBLE SECTEUR

Fig. 7.1

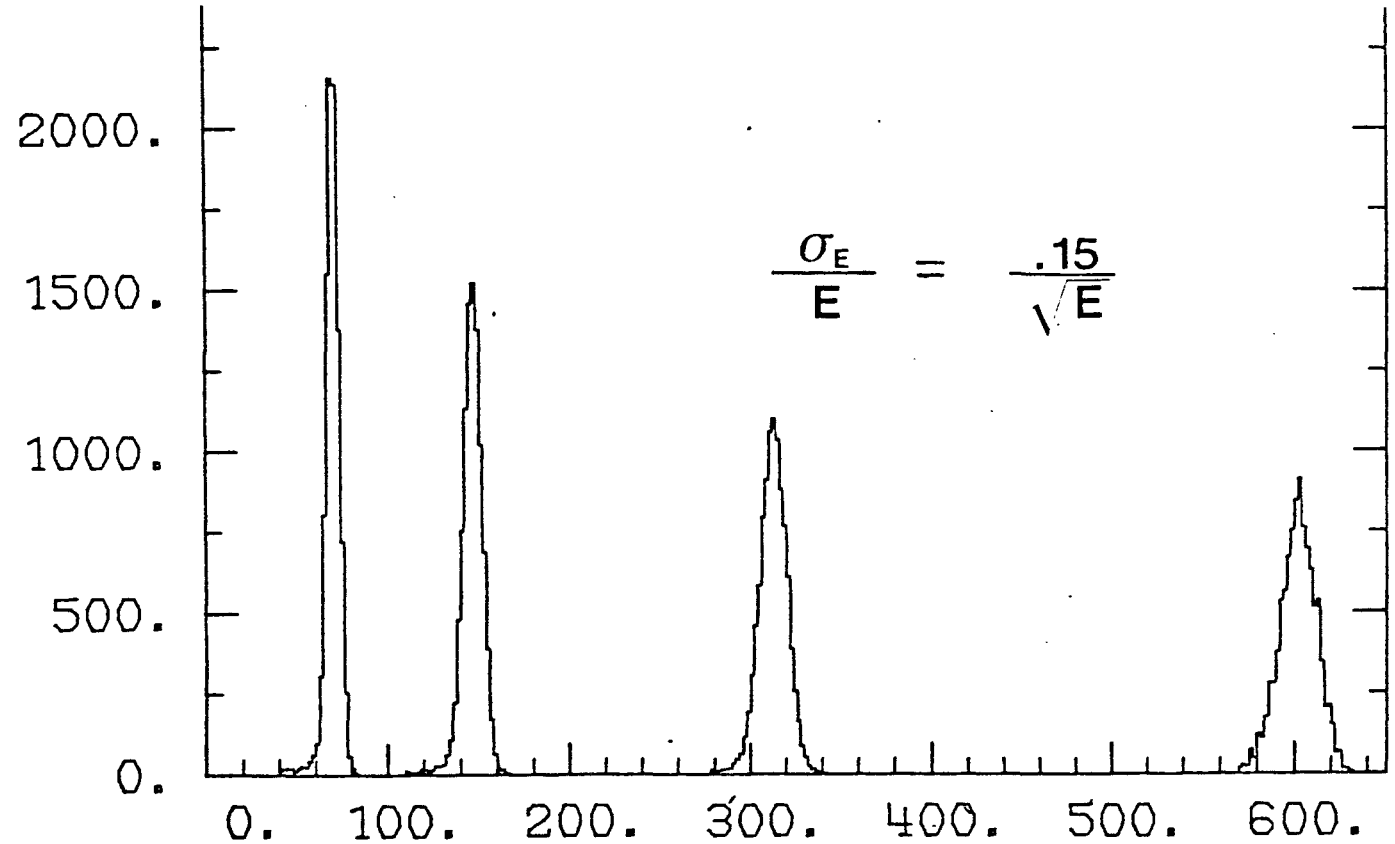
2000.
1500.
1000.
500.
0.
0. 100. 200. 300. 400. 500. 600.
$\frac{\sigma_E}{E} = \frac{.15}{\sqrt{E}}$
ADC COUNTS (ARBITRARY UNITS)

Fig. 7-2

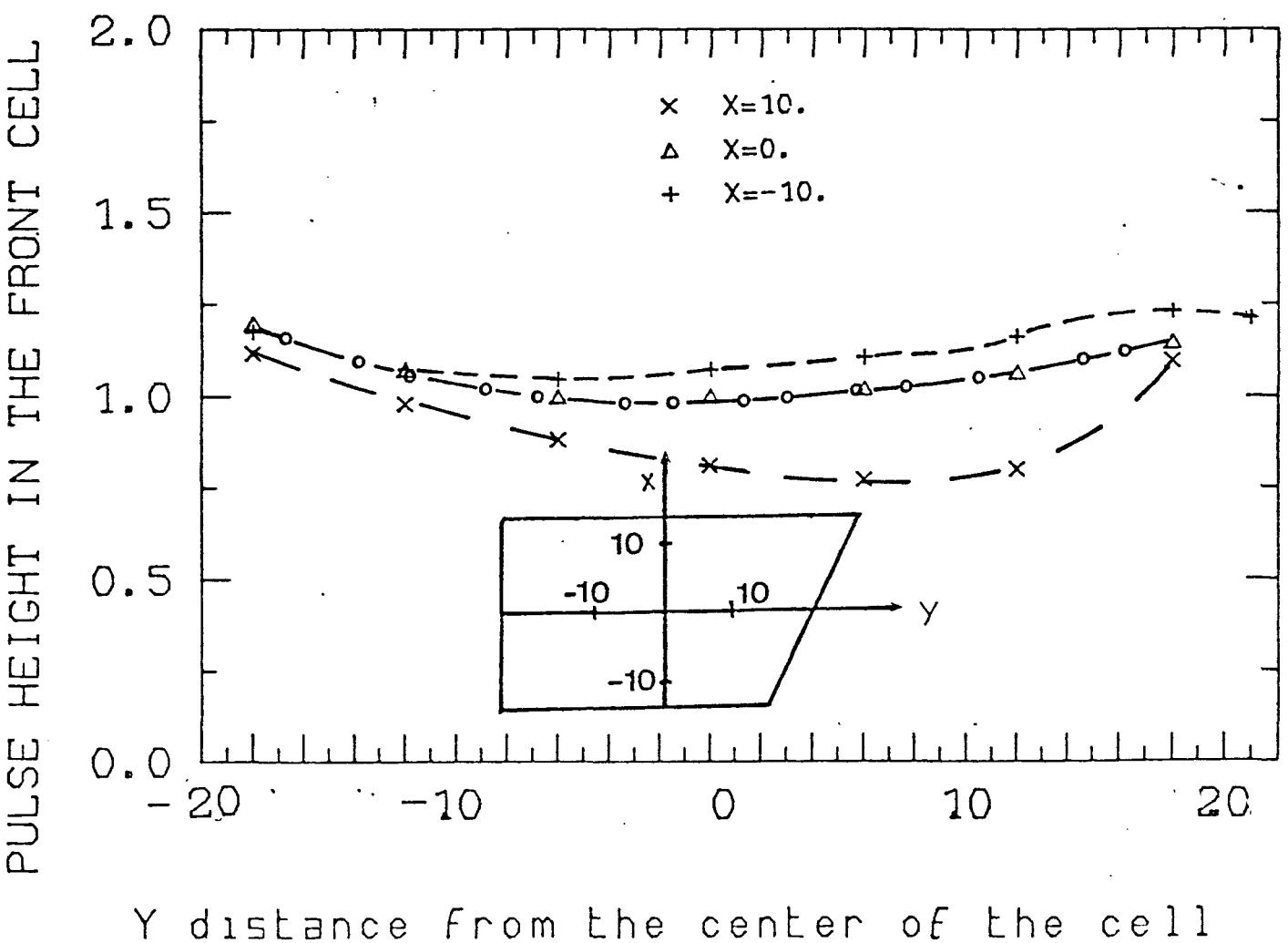
2.0
1.5
1.0
0.5
0.0
-20
-10
0
10
20
× X=10.
△ X=0.
+ X=-10.
x
10
-10
10
-10
y
PULSE HEIGHT IN THE FRONT CELL
Y distance from the center of the cell

Fig. 7-3

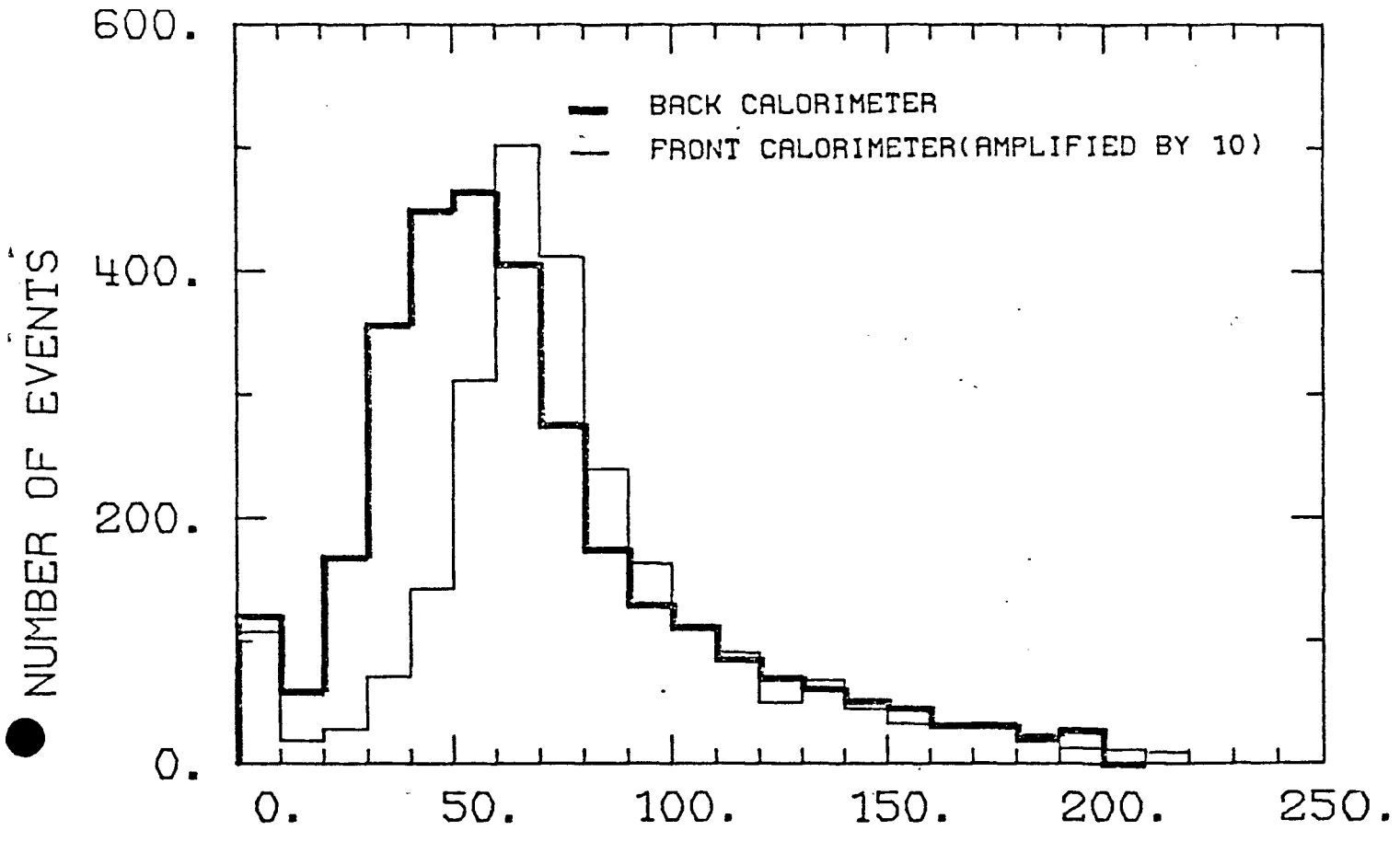
BACK CALORIMETER
FRONT CALORIMETER(AMPLIFIED BY 10)
NUMBER OF EVENTS
600.
400.
200.
0.
0.
50.
100.
150.
200.
250.
ADC COUNTS (ARBITRARY UNITS)

Fig. 7-4

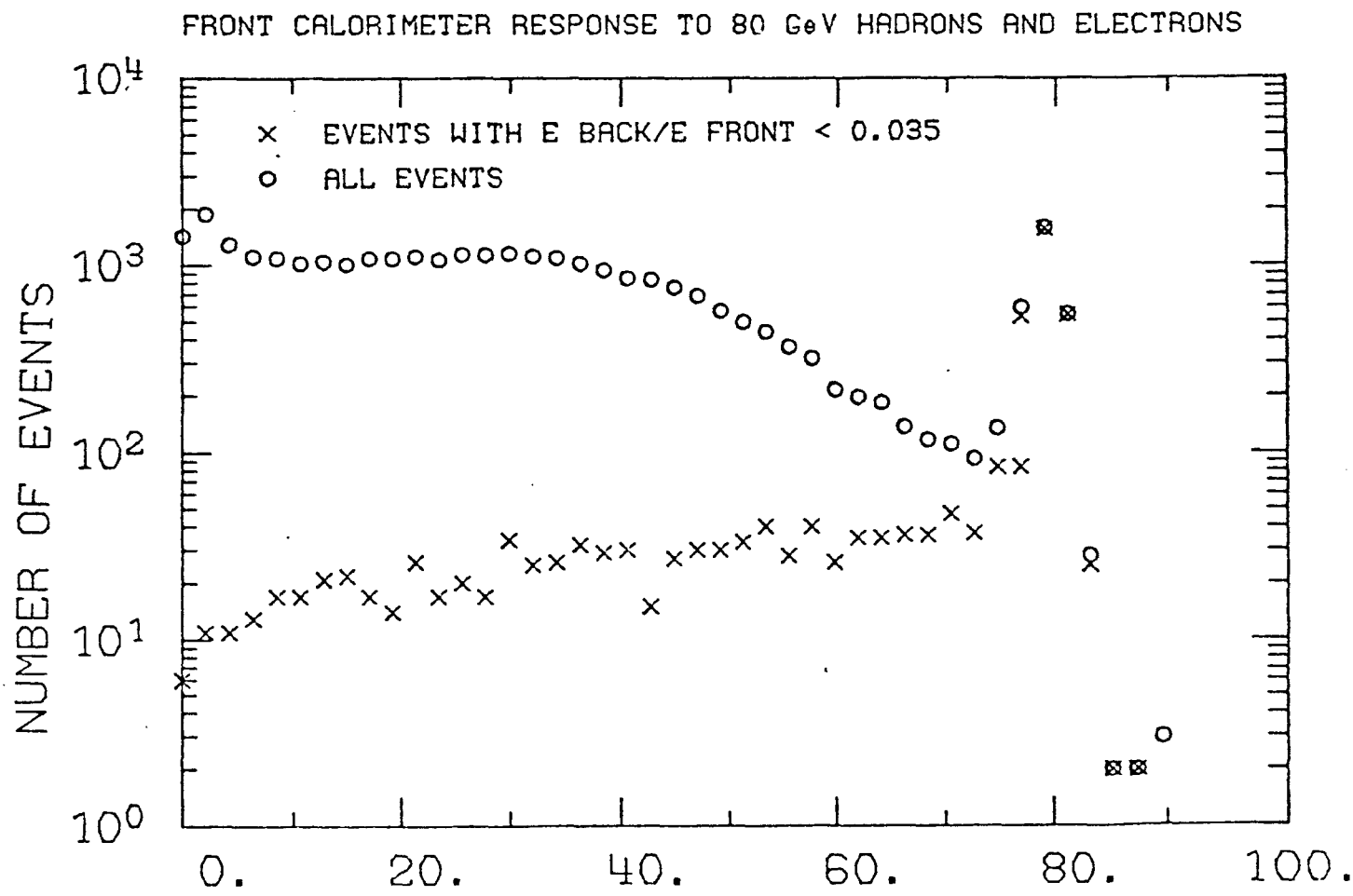
FRONT CALORIMETER RESPONSE TO 80 GeV HADRONS AND ELECTRONS
EVENTS WITH E BACK/E FRONT < 0.035
ALL EVENTS
NUMBER OF EVENTS
10^4
10^3
10^2
10^1
10^0
0.
20.
40.
60.
80.
100.
E deposited (GeV)

Fig. 7-5